Final Report:

Survey and Investigation of Buildings Damaged by Category III, IV & V Hurricanes in FY 2022-2023 - Hurricane Ian

Project #: P0091032

Submitted to:

Florida Department of Business and Professional Regulation

Mo Madani, Program Manager
Building Codes and Standards
1940 North Monroe Street
Tallahassee, Florida 32399

Prepared by:

Report No. 02-23
13 June 2023

David O. Prevatt, Ph.D., PE (MA)
Principal Investigator
Professor, University of Florida (Structures)

David B. Roueche, Ph.D.
Co-Principal Investigator
Associate Professor, Auburn University, Alabama

Kurtis R. Gurley, Ph.D.
Co-Principal Investigator
Professor, University of Florida

Engineering School of Sustainable Infrastructure and Environment
Department of Civil and Coastal Engineering
University of Florida
365 Weil Hall
P.O. Box 116580
Gainesville, FL 32611-6580

Table of Contents

1 SUMMARY OF HURRICANE IAN (2022)

On September 28, 2022, Hurricane Ian made landfall near Cayo Costa, FL as a Category 4 hurricane according to the National Hurricane Center, with peak sustained wind speeds over water estimated at 150 mph (Bucci et al. 2023), a minimum surface pressure of 940 mb, and preliminary storm surge inundation measurements of 13 ft relative to NAVD88 (USGS, 2022). The results were catastrophic in terms of both damage to infrastructure and loss of human life on the densely populated west coast of Florida, particularly in the barrier islands off Ft. Myers and Cape Coral. Tragically, Ian caused 66 direct fatalities in Florida, the highest direct loss of life in any hurricane landfalling in Florida since the 1935 Labor Day hurricane. The fatalities were primarily associated with the heavy storm-surge that struck the barrier islands of Sanibel, Ft. Myers Beach, and Bonita Beach. Nearly 50% of the victims were over 70 years of age (FMEC 2022). Wind damage was generally less severe, but widespread roof cover loss and other building envelope damage drove extensive economic losses. Widespread inland flooding due to heavy rainfall was reported across Florida and into the Carolinas as Ian made a second landfall there.

Hurricane Ian stands to be one of the costliest landfalling hurricanes of all time in the US, despite it being a below-design wind event. Risk modelers estimated wind and coastal storm surge losses of $40-$74 billion. These estimates do not include losses due to inland flooding covered by the National Flood Insurance Program (NFIP) and uninsured losses, which are likely to be high given the extensive inland flooding and low percentage of homes with flood insurance in these areas.

While making landfall in the same location as Hurricane Charley did 18 years earlier, with similar peak sustained wind speeds, damage from Charley was primarily driven by high winds concentrated within a narrow band of this relatively small hurricane. In contrast, Ian was a larger storm and as a result drove a much higher storm surge that was upwards of 13 ft above NAVD88 based on preliminary measurements. The surge impacted regions with high population densities housed in both elevated and on-grade residential structures, including mobile and manufactured home parks, along hundreds of miles of canals and coastal frontage in Cape Coral, Ft. Myers, and nearby barrier islands. Peak 3-second gust wind speeds over land, however, were less than those reported in Hurricane Charley, with the parametric wind field modeling completed by NIST/ARA estimating a peak gust of 131 mph near Punta Gorda (Figure 1). Despite the lessons on wind mitigation learned from Hurricane Charley 18 years earlier, these communities were ill-prepared for the storm surge and flooding produced by Hurricane Ian, highlighting vulnerabilities that likely exist in many similar communities along coastlines around the US.

The above summary of Hurricane Ian's impacts is adapted from a comprehensive assessment of Hurricane Ian (2022) led by the Structural Extreme Events Reconnaissance (StEER) network (Kijewski-Correa et al. 2021) which was published in the form of a Preliminary Virtual Reconnaissance Report (PVRR) (Cortes et al. 2022). The report covered the meteorological history of Hurricane Ian, observed impacts to the built infrastructure, and the regulatory context surrounding the performances. PIs Prevatt and Roueche contributed to the synthesis of knowledge and writing of the report.

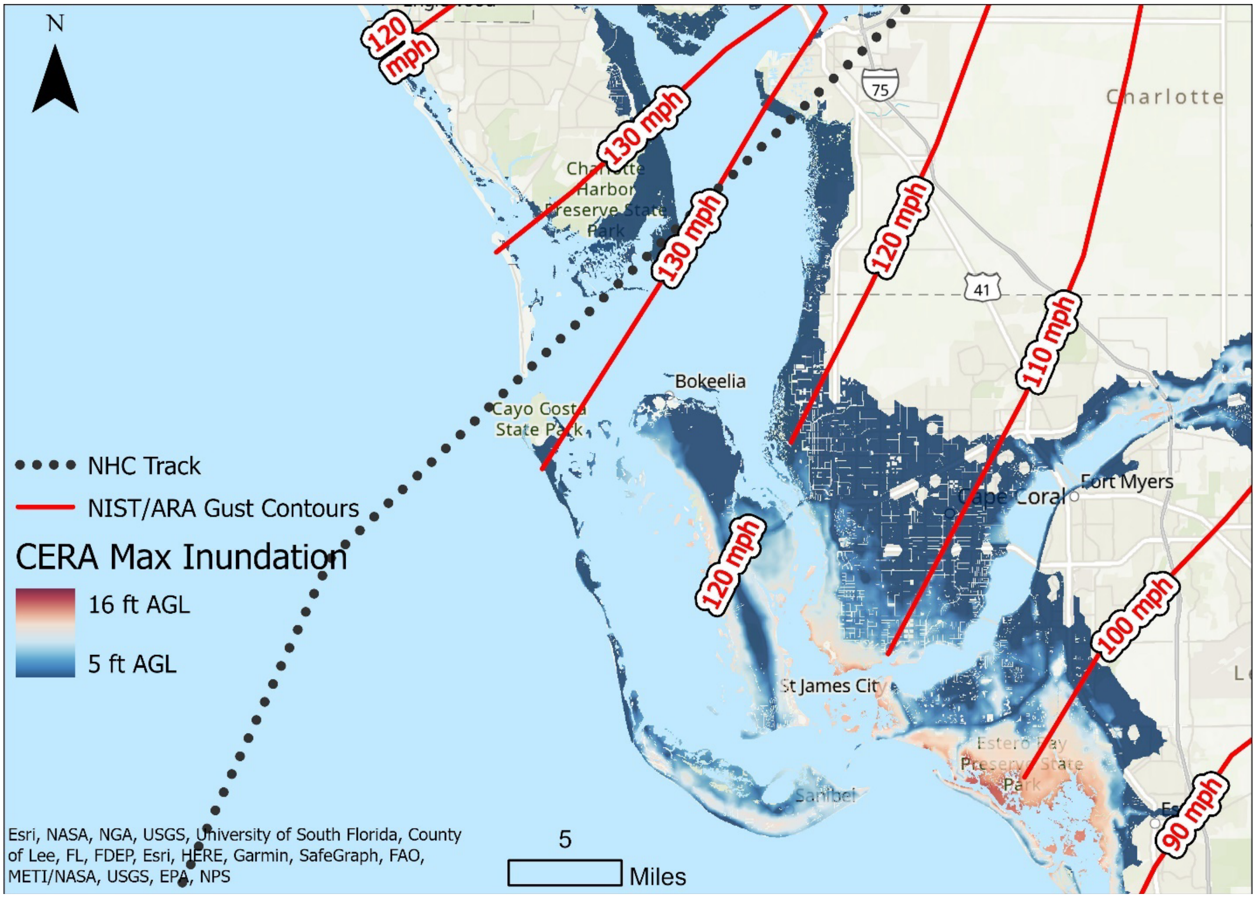

Figure 1. Peak wind and surge inundation hazards estimated from Hurricane Ian. Wind speeds represent 3-second gusts at 10 m height in open terrain and are sourced from ARA (2022). Surge inundation represents maximum still water levels above ground and are sourced from CERA (Dubrow 2020).

2 STATEMENT OF OBJECTIVES, SCOPE AND RELEVANT FBC ELEMENTS

2.1 Scope of Work

The following outlines the project scope of work and the status.

Task 1. The Contractor shall maintain data collection equipment and transport equipment as necessary for measuring intensity of land-falling hurricanes and documenting damage caused by those land-falling hurricanes.
Status: Completed.

Task 2. The Contractor may conduct one deployment training exercise (Thunderbolt Drill) in the field to ensure personnel are trained and familiarized with wind monitoring equipment and data collection procedures.
Status: Completed.

Task 3. Perform field data collection preparation to include:

- **a)** Purchase and organize data collection and recording equipment.
- **b)** Vehicle maintenance.
- **c)** Document equipment and software available for database construction.

Task 4. Organize and execute an initial triage assessment of residential property damage resulting from a Category III, IV, or V hurricane.

- **a)** Deploy wind monitoring assets in the event of a land-falling hurricane.
  Status: Two wind monitoring assets were deployed for Hurricane Ian (2022). See Appendix A.
- **b)** Provide an initial triage assessment of residential property damage, including approximate extent of visible water depths, where evident.
  Status: Completed. PI Prevatt performed triage assessments on September 29, 2022, and again on October 2-3, 2022. Assessments were presented to the Florida Building Commission in October and December meetings.

Task 5. Organize and execute a formal survey and damage assessment effort as directed and approved by the program manager. The formal damage assessment effort may include contracting with a licensed supplier of unmanned aerial vehicles to take photographs above the damaged areas.

Status: Completed.

- Observations from the triage deployments are included in the StEER Early Access Reconnaissance (EARR) report (Kijewski-Correa et al. 2023), a portion of which related to observed performance is provided in Appendix B. PIs Prevatt and Roueche also coordinated the collection of over 600 miles of surface-level panoramic imagery throughout the impacted region by StEER and independent contractor SiteTour 360, and over eight square miles of aerial imagery captured by a low-altitude UAS in collaboration with StEER and the NSF NHERI RAPID Experimental Facility (Berman et al. 2020)[1]. Each of these data sources are available to the research team for the current project.
- PI Gurley participated in a robust deployment between October 19-23, 2022, coordinated by StEER. The performance assessment team, including PI Gurley, consisted of seven practicing engineers and engineers in academia. The team assessed the performance of both residential and commercial structures primarily on Sanibel and Fort Myers Beach, conducting 274 building performance assessments in total.

The following refinements in scope to Task 5 were proposed and accepted during the presentation of the Task 4 Triage Report to the Florida Building Commission on 6 December 2022:

Task 5.1. Data Enrichment. Execute a data enrichment process to augment the triage building performance dataset using data from county Property Appraisers and other supplemental data sources not available in field to evaluate building performance relative to

a. Age
b. Edition of FBC Building Code
c. Materials (cladding and structural)
d. Location and associated hazard intensities

Status: Completed. See Sections 3-5 for details.

[1] The Natural Hazards Engineering Research Infrastructure (NHERI) RAPID Facility is funded by the National Science Foundation to provide investigators with equipment, software, and support services needed to collect, process, and analyze perishable data from natural hazard events. More information is available at https://rapid.designsafe-ci.org/.

Task 5.2. Elevated Structures. Collate evidence on performance of elevated structures and effects of buoyancy and hydrodynamic forces.
Status: Completed. See Sections 3-5 for details.

2.2 Relevance to the Florida Building Code

This project stratifies building performance by building code era, hazard intensity, first floor elevation, and other notable features to facilitate an evaluation of building performance under the latest buildings codes contrasted with those from earlier code editions. Table 1 summarizes the various editions of the Florida Residential Building Code and their effective dates.

Specific code-related topics that are evaluated include performance of breakaway walls relative to code provisions (Section R322.3.5), placement of the coastal construction control line (Section R322.1.11), evidence for surge-induced floor slab uplift forces (Section R322.3.4), and performance of common roof cover (e.g., Section R903) and wall cladding (e.g., Table R703.3(1)) elements.

Table 1. Effective dates for each version of the Florida Residential Building Code.

Edition	Code Basis	Referenced ASCE 7	Effective Date	Nominal Effective Years
2001 FBC	1997 SBC	7-98	March 1, 2002	2002-2005
2004 FRBC	2003 IRC	7-02	October 1, 2005	2006-2008
2007 FRBC	2006 IRC	7-05	March 1, 2009	2009-2011
2010 FRBC	2009 IRC	7-05	March 15, 2012	2012-2015
2014 FRBC	2012 IRC	7-10	June 30, 2015	2016-2017
2017 FRBC	2015 IRC	7-10	December 31, 2017	2018-2020
2020 FRBC	2018 IRC	7-16	December 31, 2020	2021 - current

3 PERFORMANCE ASSESSMENTS

Performance of residential buildings regulated by the Florida Residential Building Code was assessed using both on-site investigations, conducted by members of the Structural Extreme Events Reconnaissance (StEER) network, and virtual investigations, which utilized a variety of supplemental imagery and data sources described later in this report.

3.1 On-Site Performance Assessments

The on-site performance assessments were conducted by members of the Structural Extreme Events Reconnaissance (StEER) network between October 19th and November 4th, 2022. Table summarizes the deployments by personnel and objectives. PI-s Prevatt and Roueche assisted with coordinating the deployments, including selection of target buildings for assessment and sampling strategy, while co-PI Gurley deployed on-site between October 19-23 and conducted performance assessments of individual buildings. In addition to the building performance assessments, personnel also documented high water marks and conducted aerial missions with unmanned aerial systems over Fort Myers Beach and Sanibel Island to capture high-resolution oblique and nadir imagery suitable for reconstruction of 3D point clouds and high-resolution orthomosaics.

On-site performance assessments were conducted using a custom survey form developed by StEER optimized for coastal storms and deployed via smartphone app through the Fulcrum platform (Spatial Networks, 2022). The survey form facilitated the capture of geotagged photographs directly from the user's mobile device, extraction of all device-supplied metadata (date, time, etc.), and automatic geocoding of the local addresses based on GPS coordinates of the records. Investigators were also prompted to document details of the structural load path, including presence of breakaway walls and other coastal features, and define the observed exterior damage to fenestration, wall cladding, roof cover, and structural systems. Due to time constraints, typical assessments primarily consisted of detailed photographs and a few notes on the structural system and load path, and key damage observations. Most of the 275 on-site assessments documented the performance of residential structures, but commercial and critical facilities were also a focus of the StEER mission.

In coordination with the building performance assessments, two coastal survey teams also documented High Water Marks (HWM) and wave elevation estimates throughout Sanibel and Fort Myers Beach. In total, the team collected 179 records. HWM were georeferenced to the NAV88 vertical datum using a Leica GS-18 GNSS RTK Rover. After post-processing, the final values were provided as HWM Elevation above Mean Sea Level (MSL), HWM Elevation above NAV88, Flow Depth Over First Floor (if HWM was taken at a building), Flow Depth Over Grade Level, and (at select locations) Wave Height. More details on the coastal survey methods are provided in Alam et al. (n.d.).

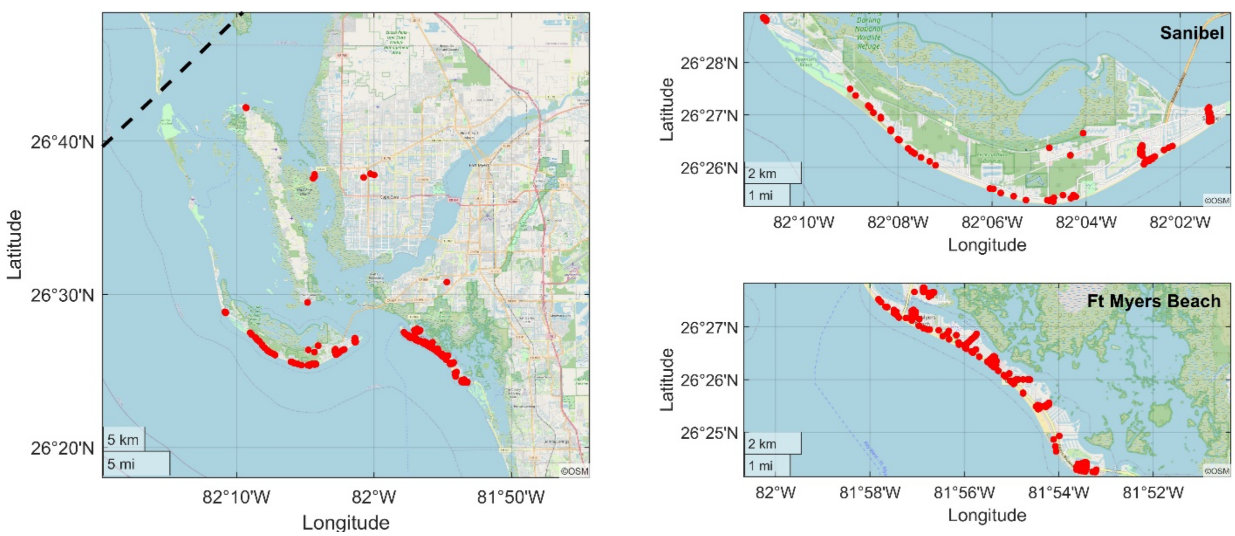

Figure 2. Locations of on-site performance assessments collected by StEER.

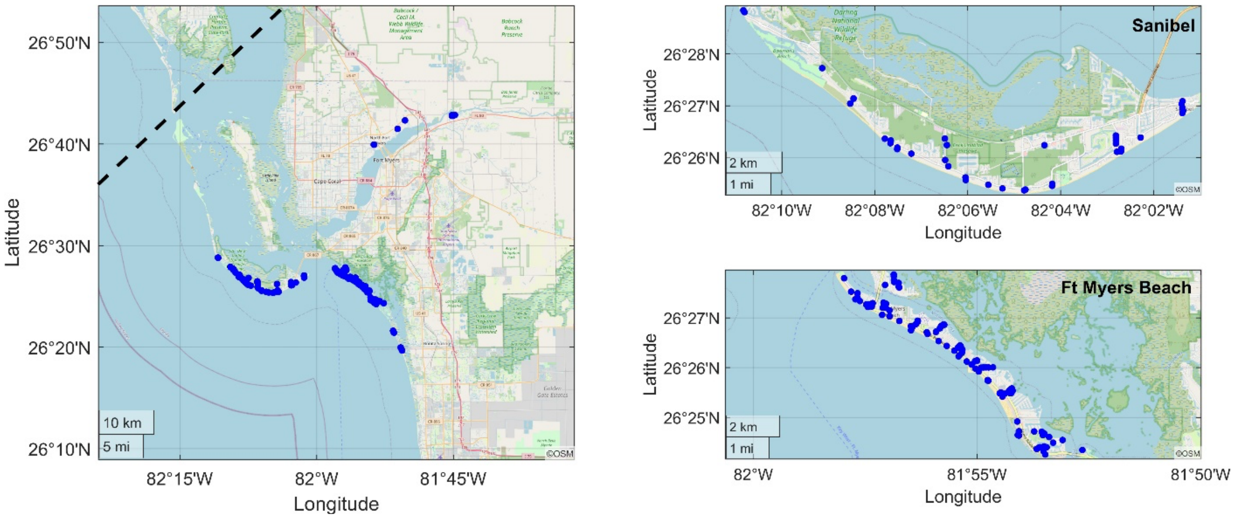

Figure 3. Locations of HWM assessments collected by StEER.

3.2 Virtual Performance Assessments

The on-site building performance assessments collected by StEER primarily consisted of structures exposed to coastal hazards in Sanibel and Ft. Myers Beach. To supplement these efforts and build out a more representative wind hazard performance dataset, a stratified, random sample set was selected within a domain of buildings in Lee and Charlotte counties that were adjacent to and visible in the post-Ian street-level panoramic imagery captured by StEER and SiteTour 360 (Figure 4). Residential buildings within this domain were stratified across the following dimensions:

- Occupancy type (Single Family, Multi-Family (including Condominiums))
- Code era of construction (pre-2002, 2003-2005, 2006-2010, 2011-2017, 2018-2022)
- Hurricane Ian wind zone (80-99, 100-109, 110-119, 120-131 mph maximum 3 second gust).
- Proximity to high water mark (within 50 ft, outside of 50 ft).
- Samples were drawn such that, if available, there were approximately 15 single-family residential and 5 multi-family residential buildings in each sample class.

To perform the stratified sampling, occupancy type and year of construction were taken from the Lee and Charlotte County property appraiser datasets. Hurricane Ian wind speeds were sourced from the ARA/NIST wind maps. High water mark locations were based on measurements taken by both StEER and the United States Geological Survey (USGS 2022).

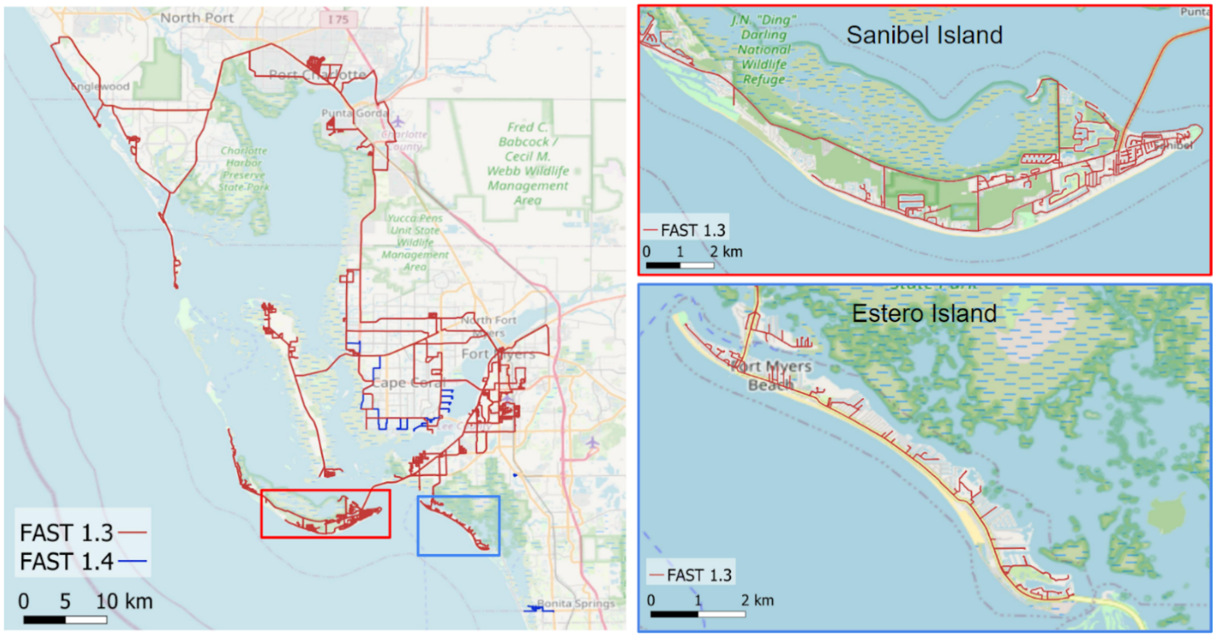

Figure 4. Routes along which street-level panoramic imagery was capturing post-Hurricane Ian by StEER Field Assessment Structural Teams (including SiteTour 360 as FAST 1.3).

3.3 Characteristics of Buildings in the Combined Performance Assessment Dataset

The virtual assessments in combination with the on-site assessments provided a representative sample inventory (illustrated in Figure 5) from which to investigate both wind and surge impacts from Ian across a variety of relevant building attributes and other characteristics. How these various characteristics were assigned is summarized in Section 4.

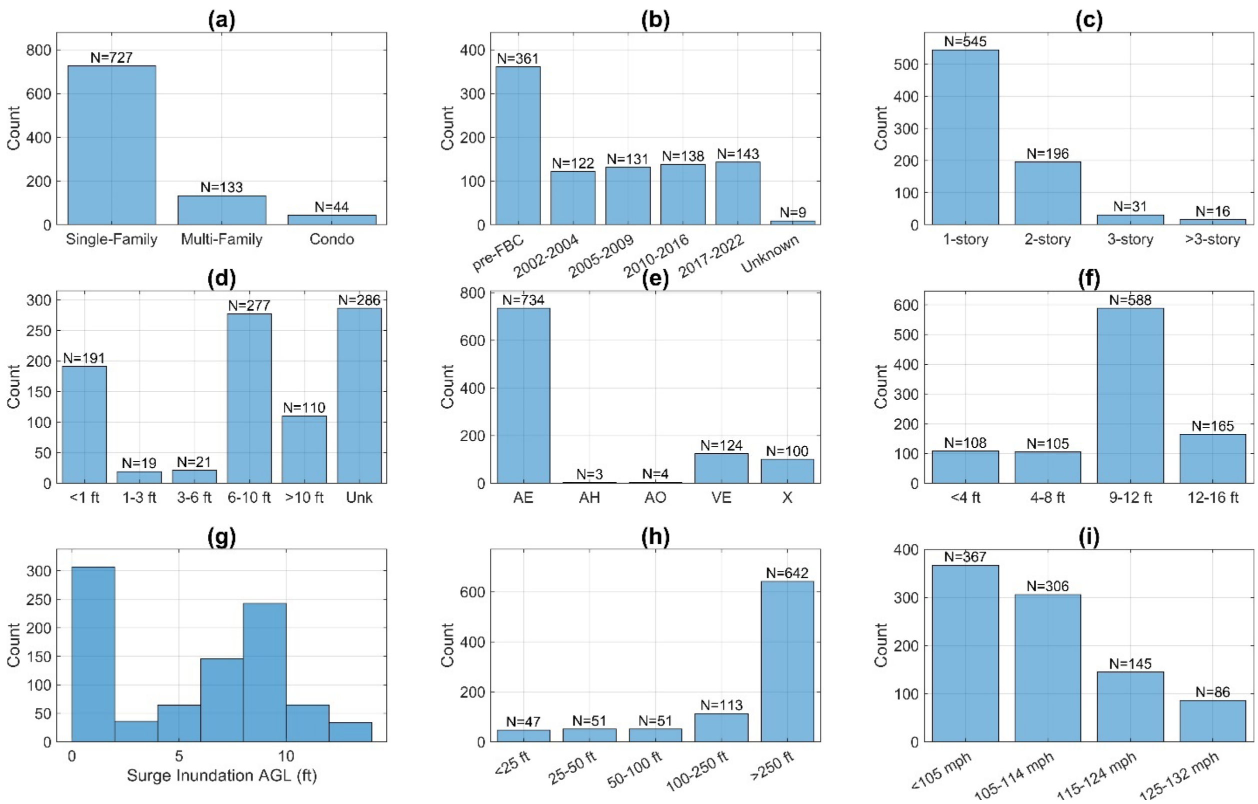

Figure 5. Distribution of samples across various stratification levels, including (a) occupancy class, (b) construction era, (c) number of stories, (d) elevation to lowest horizontal structural member, (e) FEMA flood zone based on FIRM maps, (f) base flood elevation from FIRM maps, (h) distance to nearest high water mark, and (i) estimated 3-second gust wind speeds (33 ft height, open terrain), taken from ARA (2022).

4 DATE ENHANCEMENT AND QUALITY CONTROL

The objective of the data enhancement and quality control (DEQC) process is to (1) bring as many assessments as possible up to a common level of attributes and features (listed in Appendix E), and (2) minimize the number of errors in the final dataset used for analysis. To accomplish this objective required the synthesis of many different data sources (Table 2) through both manual and automated procedures. Manual procedures were primarily completed by a team of trained graduate and undergraduate engineering students at Auburn University and the University of Florida. Methodologies for obtaining select features are described in the following sections.

Table 2. Primary data sources in use for performing data enrichment and analysis tasks.

Name	Provider	Data Class	Description	Use to Project
StEER Performance Assessments	Structural Extreme Events Reconnaissance Network	Performance Assessments	On-site post-Ian photographs and basic attributes for select buildings	Starting point for data enhancement
StEER High Water Marks	Structural Extreme Events Reconnaissance Network	Hazard Intensity	High water marks documenting surge inundation throughout the landfall region	Associate observed storm surge with building performance
StEER Surface-Level Panoramas	Structural Extreme Events Reconnaissance Network / SiteTour 360	Imagery	650+ miles of street-level panoramic imagery captured post-Ian	Classify building performance and building attributes
StEER UAS Imagery	Structural Extreme Events Reconnaissance Network / NHERI RAPID EF	Imagery	High-resolution, low-altitude nadir and oblique post-Ian aerial imagery and associated products (3D models, orthomosaics)	Classify building performance and building attributes
USGS High Water Marks	United States Geological Society	Hazard Intensity	High water marks throughout the affected regions	Associate storm surge with building performance
CERA Surge Hindcast	Coastal Emergency Risk Assessment	Hazard Intensity	Surge inundation AGL obtained from a best-track hindcast of Hurricane Ian using ADCIRC.	Associate storm surge with building performance
Wind Maps	ARA, NIST, FEMA	Hazard Intensity	Interpolated 3-s gust and 1-min sustained wind speeds, standardized to 10 m height and open terrain, throughout the affected regions	Associate estimated wind speeds with building performance
Hurricane Ian Aerial Imagery	National Oceanic and Atmospheric Administration	Imagery	Post-Ian nadir imagery	Classify building performance and building attributes
LCPA Pictometry	Lee County Property Appraiser	Imagery	Pre- and post-Ian, high-resolution, nadir and oblique imagery for Lee County	Classify building performance and building attributes
Lee County Parcel Data	Lee County Property Appraiser	Public Records	Public parcel data for Lee County	Define common building attributes
Lee County Building Footprints	Lee County GIS Department	Public Records	Building footprint polygons and select associated building attributes	Automated evaluation of select building attributes
Lee County Permits	Lee County Permit Office	Public Records	Public permit information for homes in Lee County	Identify retrofits and repairs
Charlotte County Parcel Data	Charlotte County Property Appraiser	Public Records	Public parcel data for Charlotte County	Define common building attributes
Charlotte County Building Footprints	Microsoft	Public Records	Building footprint polygons for Charlotte County	Automated evaluation of select building attributes
Charlotte County Permits	Charlotte County Permit Office	Public Records	Public permit information for homes in Charlotte County	Identify retrofits and repairs
FIRM Maps	FEMA / FL Geographic Database Library	Hazard Vulnerability	GIS file containing FIRM data for Lee and Charlotte Counties.	Source of flood zones and base flood elevations
National Lidar Project	United States Geological Survey / Multiple	Digital Twin	Lidar point clouds and derived products covering Lee and Charlotte Counties	Automated evaluation of select building attributes

4.1 Elevation to Lowest Horizontal Structural Member

The Elevation to Lowest Horizontal Structural Member defines the height in feet of the lowest horizontal member of the elevated floor relative to the average ground plane elevation around the building. To estimate the ELHSM required first determining whether a building was elevated or not. For structures with breakaway walls that failed during the storm or with only partial enclosures below the elevated floor, the determination of whether it was elevated or not was relatively straightforward. For other structures, a combination of pre-Ian street-level imagery from Google Street View (looking for features such as exterior stairs extending to an elevated floor), checking county records (specifically number of stories and floorplan layouts), real estate records, and elevation certificates where present was used to evaluate whether the first finished floor was elevated or not. The level of confidence in this evaluation was generally high based on the available information.

If a home was assessed as having an elevated first floor, the height to the first floor above grade was typically estimated using the Pictometry Eagleview platform, which allows for height measurements to be made as illustrated in Figure 6. These measurements were spot-checked with elevation certifications or on-site measurements where available and found to be in good agreement within approximately +/- 1 ft.

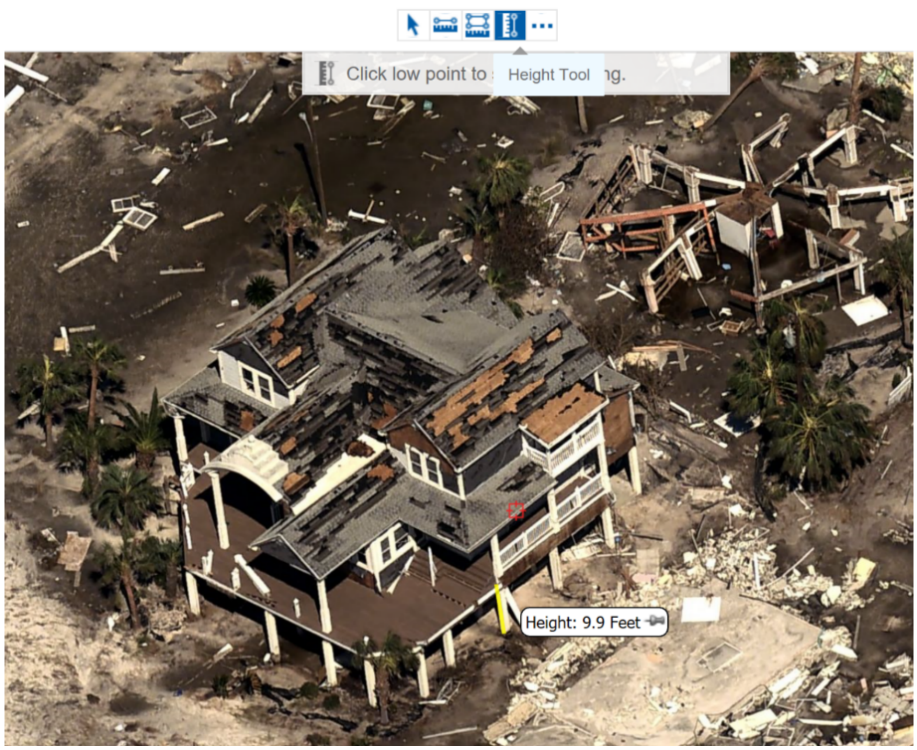

Figure 6. Measuring elevation to lowest horizontal structural member in Pictometry Eagleview.

4.2 Presence and Failure of Breakaway Walls

A breakaway wall is defined as a wall that is not part of the structural support of the building and is intended, through its design and construction, to collapse under specific lateral loading forces, without causing damage to the elevated portion of the building or supporting foundation system. The presence and performance of breakaway walls was evaluated by assigning one of the values given in Table 3. Partial failures were of particular importance as the remaining walls may have contributed additional lateral forces to the structure beyond those intended. These values were assigned by manually inspecting imagery of buildings with elevated floors. The default assumption was that ground floor enclosures around buildings with elevated floors were intended to be breakaway walls unless there was compelling evidence from the elevation certificate that this was not the case. The on-site photographs taken by StEER members and the pre- and post-Ian street-level panoramic imagery were found to be the most helpful in evaluating breakaway walls.

Table 3. Field values and meanings for evaluating breakaway wall performance.

Value	Meaning
Yes	Breakaway walls were present at the home and were damaged during the storm.
Yes – partially	Breakaway walls were present at the home and were damaged, but did not completely fail, or only portions of the wall along any one dimension of the home failed.
No	Breakaway walls were present at the home but were not visibly damaged during the storm.
Possibly	Breakaway walls were present at the home and were possibly damaged during the storm, but damage cannot be conclusively determined.
Not Applicable	No breakaway walls were present at the home.
Unknown	It is unknown whether breakaway walls were present or not.

4.3 Debris Impact Damming

Debris impact damming was defined as the damming of loose debris, carried by storm surge, against the structures of homes. When the loose debris bears on the structure, it can increase the lateral loads on the structure due to the moving water acting on the loose debris, and the debris transferring those forces to the structure. Debris impact damming was evaluated using one of the following values: Yes, No, Possibly, Not Applicable, or Unknown. It was primarily assessed using post-Ian aerial imagery collected within a few days of landfall.

Figure 7. Debris damming against homes.

4.4 Exterior Wall Cladding

The exterior wall cladding defines the outermost layer of the walls, often termed the façade. It is important to keeping wind-driven rain from entering the building through the walls, and also directly impacts the economic losses associated with the building when the cladding fails. Finally, failed wall cladding can become wind-borne debris that causes further damage to other structures downwind of the source structure.

Building on recommendations from previous post-storm reconnaissance reports (Prevatt and Roueche 2019), both primary and secondary wall cladding types were identified in this study, along with the approximate proportion of total wall area each occupied on the subject structure, and the percentage of each type that was damaged or missing from the walls. Many buildings have more than one wall cladding type present, and this allowed performance of the dominant types present to be more precisely quantified.

Wall cladding was primarily assigned by reviewing pre- and post-Ian ground-level imagery, including pre- and post-Ian street-level panoramic images (e.g., Figure 8), and the on-site photographs taken by StEER members. Where these image sources were unavailable or inconclusive, county data or real estate records were also sourced to confirm or identify the wall cladding types.

Figure 8. Common wall cladding types, including (left) vinyl siding, (middle) fiber-cement board on elevated floor with stucco on ground floor enclosure, and (right) stucco.

4.5 Roof Cover

Roof cover defines the outermost layer of the roof, and in residential structures typically consists of asphalt shingles, clay or concrete tiles, or standing seam metal roof panels. For this study, the roof cover type and damage ratio was defined. Roof cover type was assigned by reviewing high-resolution pre- or post-Ian aerial imagery (Figure 9) and selecting the best option from a list of pre-defined options that included laminated asphalt shingles, 3-tab asphalt shingles, clay tiles, concrete tiles, metal shingles, corrugated metal panels, standing seam metal panels, built-up roofs, and more.

Figure 9. Examples of common roof cover types identifiable from pre- or post-Ian aerial imagery, including (left) laminated asphalt shingles, (middle) clay tiles, and (right) standing seam metal roof. All images sourced from Pictometry Eagleview.

4.6 Component-level Damage Quantification

Damage to individual building components was primarily quantified by damage ratios, which are an estimate of the percentage of the building component that is visibly damaged or missing from the building (Figure 10). Building components included roof and wall structure (primary framing elements), roof and wall substrate (typically roof decking and wall sheathing panels), roof cover and wall cladding, and fenestration (doors and windows). Any elements missing or detached from the building were assumed damaged. For example, if half of the roof structure was missing, at least half of the roof substrate and roof cover were also assumed to be missing. In reality, portions or all of the roof substrate or roof cover may have stayed attached to the roof structure as it failed. Subsequently, substrate and cladding/cover component-level damage ratios as given should be treated as upper-bounds of the true damage ratio. Roof-related component-level damage ratios were estimated by reviewing post-Ian high-resolution aerial imagery. Wall-related component-level damage ratios were estimated using the ground photos taken by StEER members and the street-level panoramas captured by StEER and SiteTour 360.

Figure 10. Illustrative component-level damage ratios for roof cover (blue), roof substrate (yellow), and roof structure (orange). The (left) undamaged, (middle) damaged, and (right) annotated images all use Pictometry EagleView for the base image.

In addition to the roof, wall and fenestration component-level damage ratios, this study also specifically identified whether buildings have been shifted off the foundation, whether garage doors were present and, if so, damaged, whether sunrooms were present and, if so, damaged, and finally whether solar panels were present, and if so, were damaged.

4.7 Wind and Surge Damage Ratings

In addition to quantifying the performance of individual building components, overall wind and surge damage ratings were also assigned. The wind and surge damage ratings are as defined in Kijewski-Correa et al. (2020), and are also provided in Appendix D. In areas of significant surge, where buildings were completely washed away, wind damage ratings were not assigned. Conversely, in areas where the surge hazard was insignificant for structural loading (broadly defined as areas outside Sanibel, Fort Myers Beach, and San Carlos Island), surge damage ratings were not assigned.

4.8 Leveraging Automation for Building Attributes

Automation was leveraged where possible to improve the efficiency of collecting building attributes important to the study, including geometry, year of construction, and occupancy. Geometric building attributes, including the length, width, and mean roof height, are important features in estimating the wind and surge loads acting on the structure. An automation procedure was used in this study to minimize the manual efforts required. Here length is defined as the maximum distance across the building footprint, and the width the minimum distance across the building footprint along a dimension orthogonal to the length. Mean roof height is the average height of the roof relative to ground level or a standard vertical datum. These attributes were obtained by developing an automated procedure in Python that leverages an existing national Digital Elevation Model provided by the USGS, Digital Surface Models from lidar datasets also provided by the USGS, and building footprints sourced from the Lee County GIS department and the Microsoft Building Footprints database (Figure 11). The building length and width were calculated from a bounding box fit around each building footprint. The mean roof height was calculated by first calculating the 60th percentile elevation of the DSM within each building footprint relative to the NAV88 vertical datum. Secondly, the ground elevation at each building location (also relative to NAV88) was obtained by querying the elevation from the USGS Point Elevation Query (https://apps.nationalmap.gov/epqs/). Finally, the ground elevation was subtracted from the 60th percentile elevation from the DSM to obtain the mean roof height estimate. This procedure was performed for approximately 70% of the full dataset with good results (Figure 12); the remaining 30% were not able to be obtained in this way due to several factors, due to the DSMs (collected in 2018) not including the more recently constructed buildings, and the building footprints datasets not containing some of the most recently constructed buildings.

In addition to the geometric attributes, year of construction and occupancy was sourced from the Florida parcel dataset compiled and hosted by the Florida Geographic Data Library using a spatial join between the point location of the building and the boundaries of the parcel (from the Florida parcel dataset) for each building.

Figure 11. Building footprints overlaid on a digital surface model for an illustrative region on Fort Myers Beach. Red circles indicate structures in the sample study dataset described in this report.

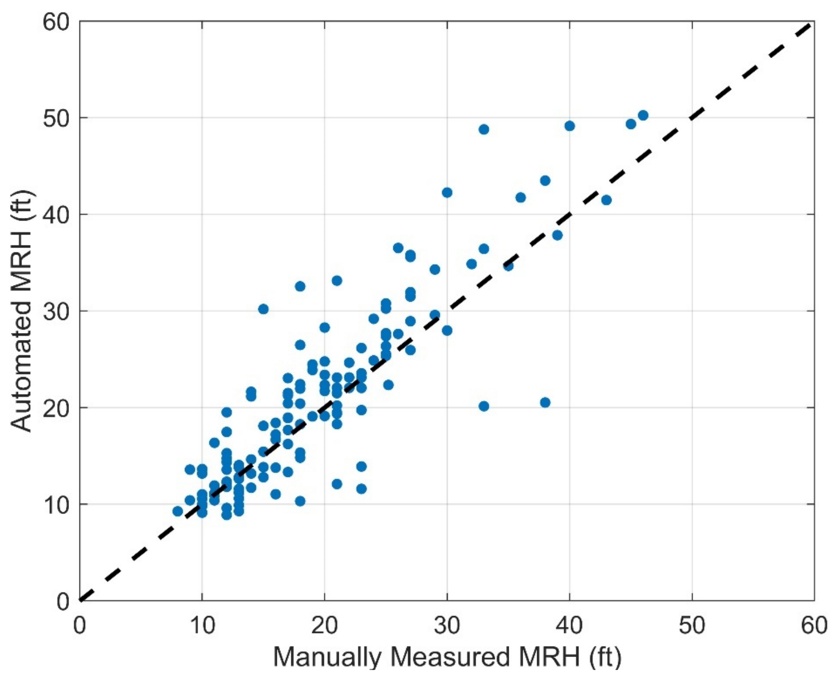

Figure 12. Illustrative match between measured and automated estimates of the mean roof height for a sample set of 133 buildings.

5 PERFORMANCE OF BUILDINGS SUBJECTED TO COASTAL HAZARDS

The evaluation of buildings subjected to coastal hazards focused on buildings in Sanibel and Fort Myers Beach. Out of the study dataset, 430 residential buildings were in these two locations. Both islands are relatively low-lying. A few areas, including the coastal roads of Estero Blvd in Fort Myers Beach and Gulf Drive in Sanibel, sit at elevations closer to 6-7 ft. But most of the occupied areas of the islands have bare-earth elevations of 3-4 ft relative to NAV88 based on the 2018 digital elevation model. As such, buildings on the islands are vulnerable to flood hazards, and most areas of the islands are subsequently within the FEMA flood zones of AE (82% of buildings) and VE (17% of buildings), indicating high flood hazard risk.

While both islands are vulnerable to flood hazards, Sanibel is less so due to some natural features. For one, structures along the coast of Sanibel are typically set back further from the mean tide level than those on Fort Myers Beach. Further, Sanibel's beaches and the island overall has much greater coverage of trees and shrubs than Fort Myers Beach (Figure 14), which can mitigate the wave impacts and flow velocity of storm surge.

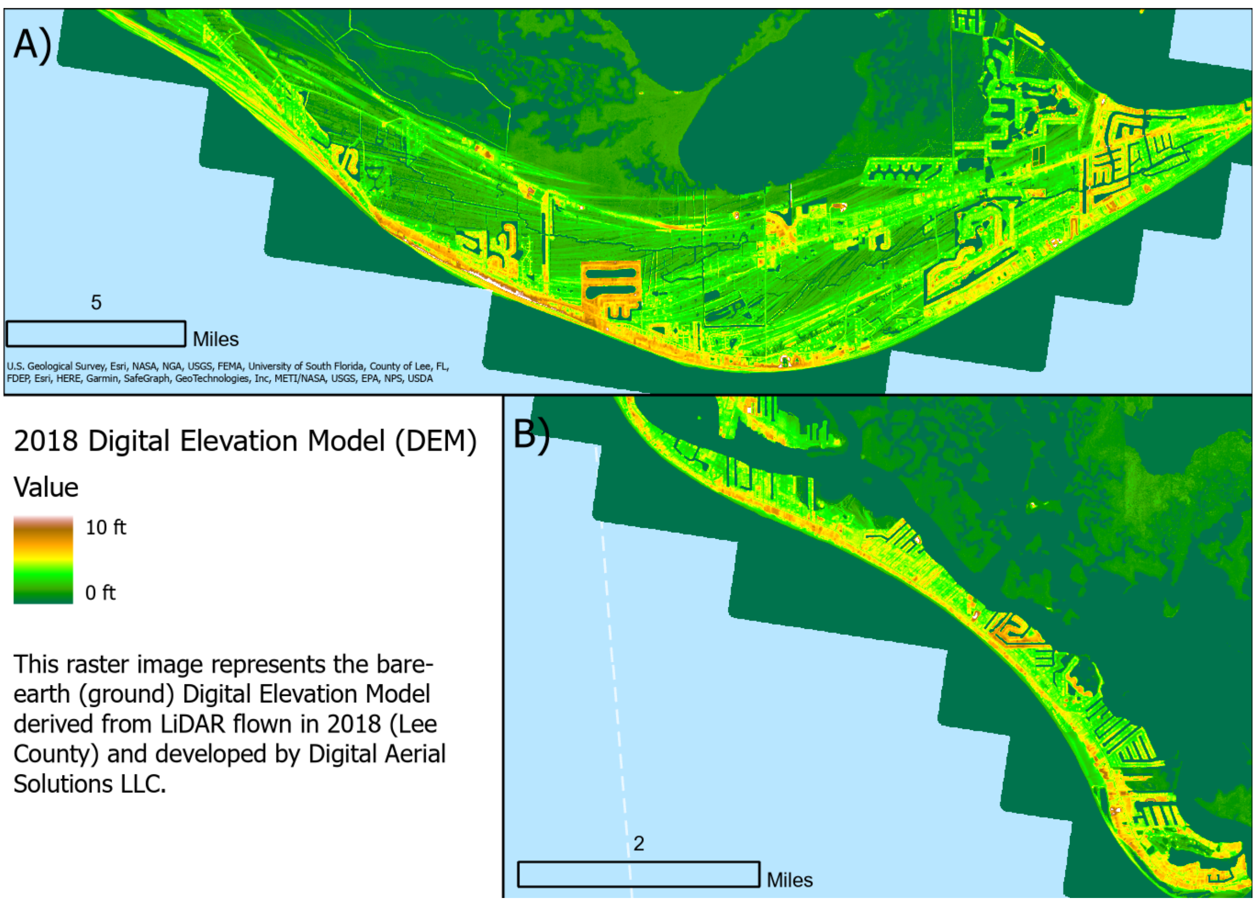

Figure 13. Bare earth Digital Elevation Model for (A) Sanibel and (B) Fort Myers Beach.

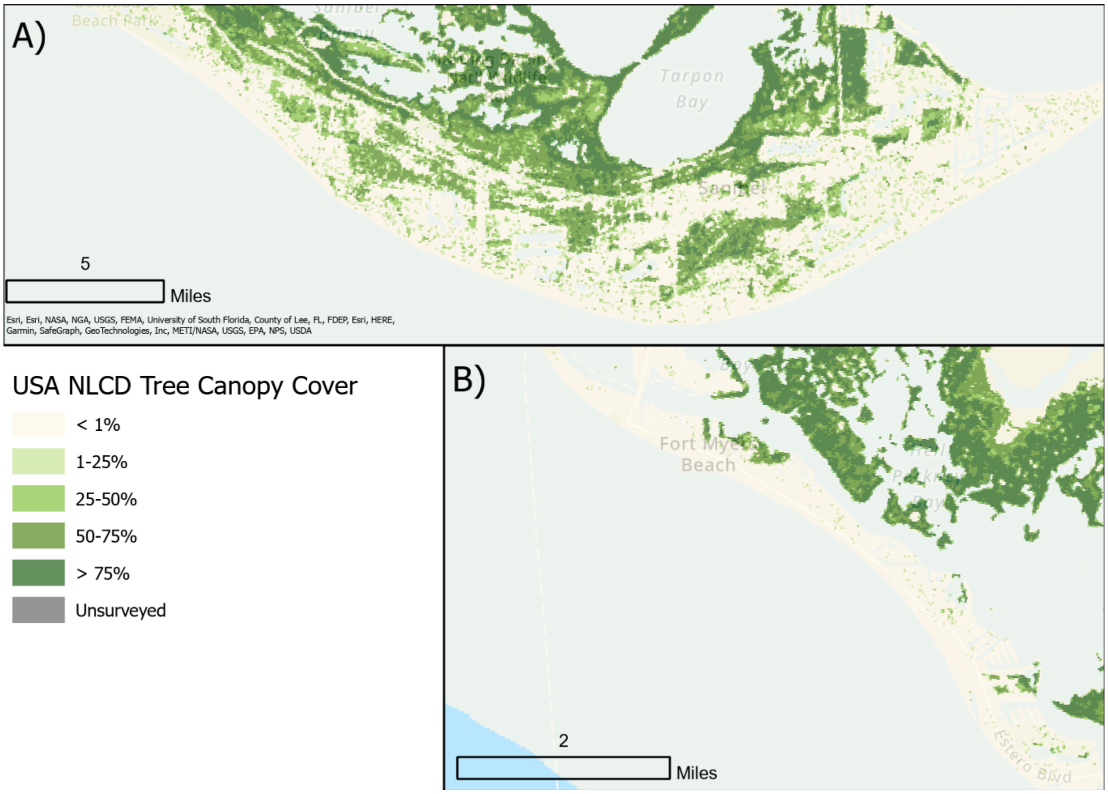

Figure 14. Tree canopy cover in (A) Sanibel and (B) Fort Myers Beach from the National Land Cover Dataset (Wickham et al. 2014), showing a greater prevalence of vegetation on Sanibel than on Fort Myers Beach.

5.1 Overall Performance

The overall performance of buildings subjected to coastal hazards is evaluated using the surge damage rating (SDR), which classifies the level of visible, exterior damage to the structure. Out of the 430 structures in the study dataset subjected to significant surge hazards, nearly 6% were assigned surge damage ratings of 5 or 6, which indicate major structural damage or complete collapse (Figure 15). The majority (54%) had no visible exterior surge-induced damage (SDR = 0), and 24% only experienced the loss of the breakaway walls (SDR = 1). Surge-induced damage was more severe on Fort Myers Beach than on Sanibel Island, as evidenced by approximately 8% of the study dataset on Fort Myers Beach being assigned an SDR of 5 or higher, compared to 4% for Sanibel. Further, 70% of the study dataset on Sanibel Island experienced no visible surge-induced damage (SDR = 0), compared to just 42% of structures on Fort Myers Beach. Sanibel and Fort Myers Beach had similar levels of vulnerability, with average years of construction were 1990 and 1994 respectively. Seaward of the Costal Construction Control Line (CCCL) specifically, the average years of construction were 1987 and 1996 respectively.

The spatial distribution of surge damage ratings relative to the FEMA flood zones (Figure 16) and the estimated surge hazard levels (Figure 17) shows a higher prevalence of surge-induced damage in structures located closest to the coastline. Structures in flood zone VE had an average surge damage rating of 2.4, while those in flood zone AE had an average surge damage rating of 0.7. Further, structures located seaward of the CCCL had an average surge damage rating of 2.2 compared to 0.6 for those landward of the CCCL. This is anticipated, as surge damage ratings of 1 and 2 primarily correspond to the failure of breakaway walls, which is the expected and desired response under high flood hazards, particularly under the breaking wave action that structures close to the coast would have been subjected to.

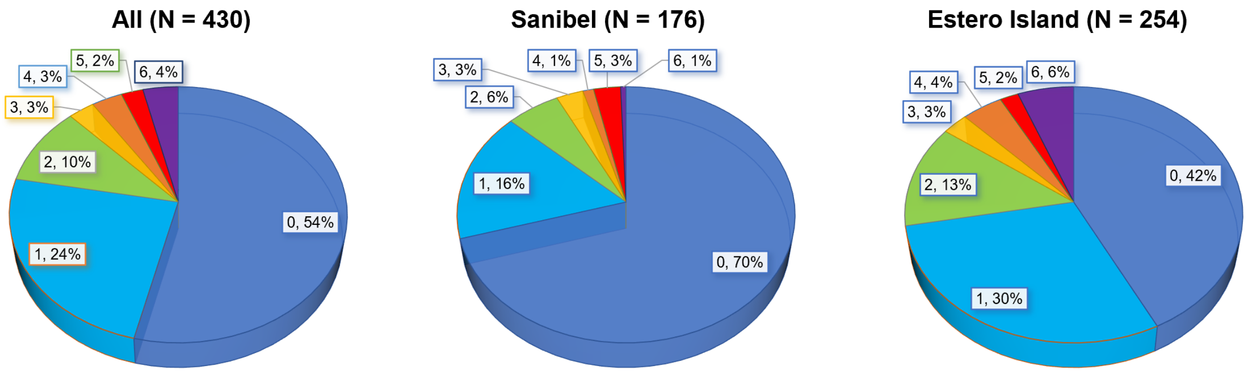

Figure 15. Distribution of surge damage ratings in the study dataset. The first number in each label is the surge damage rating, and the second is the percentage of structures in the study dataset assigned the respective rating.

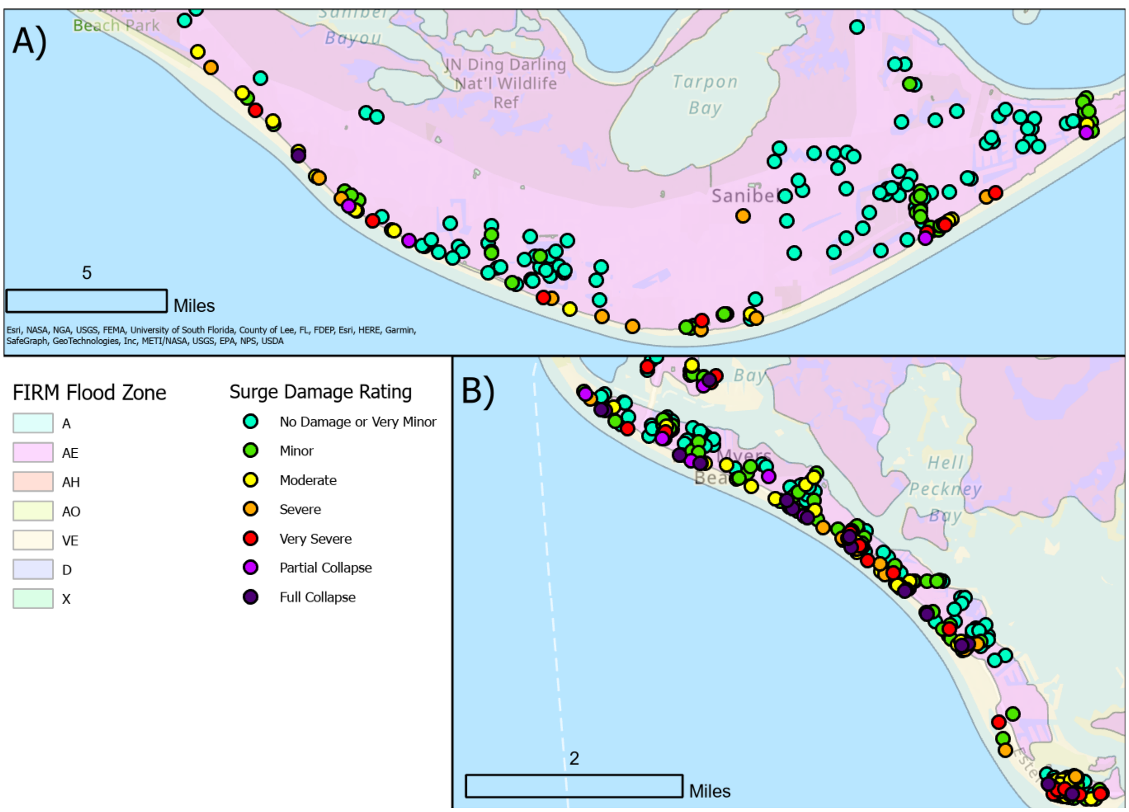

Figure 16. Spatial distribution of surge damage ratings in (A) Sanibel and (B) Fort Myers Beach with respect to the FIRM flood zones. Source: statewide FIRM GIS layer compiled by the Florida Geographic Data Library, using data sourced from FEMA as of December 2022.

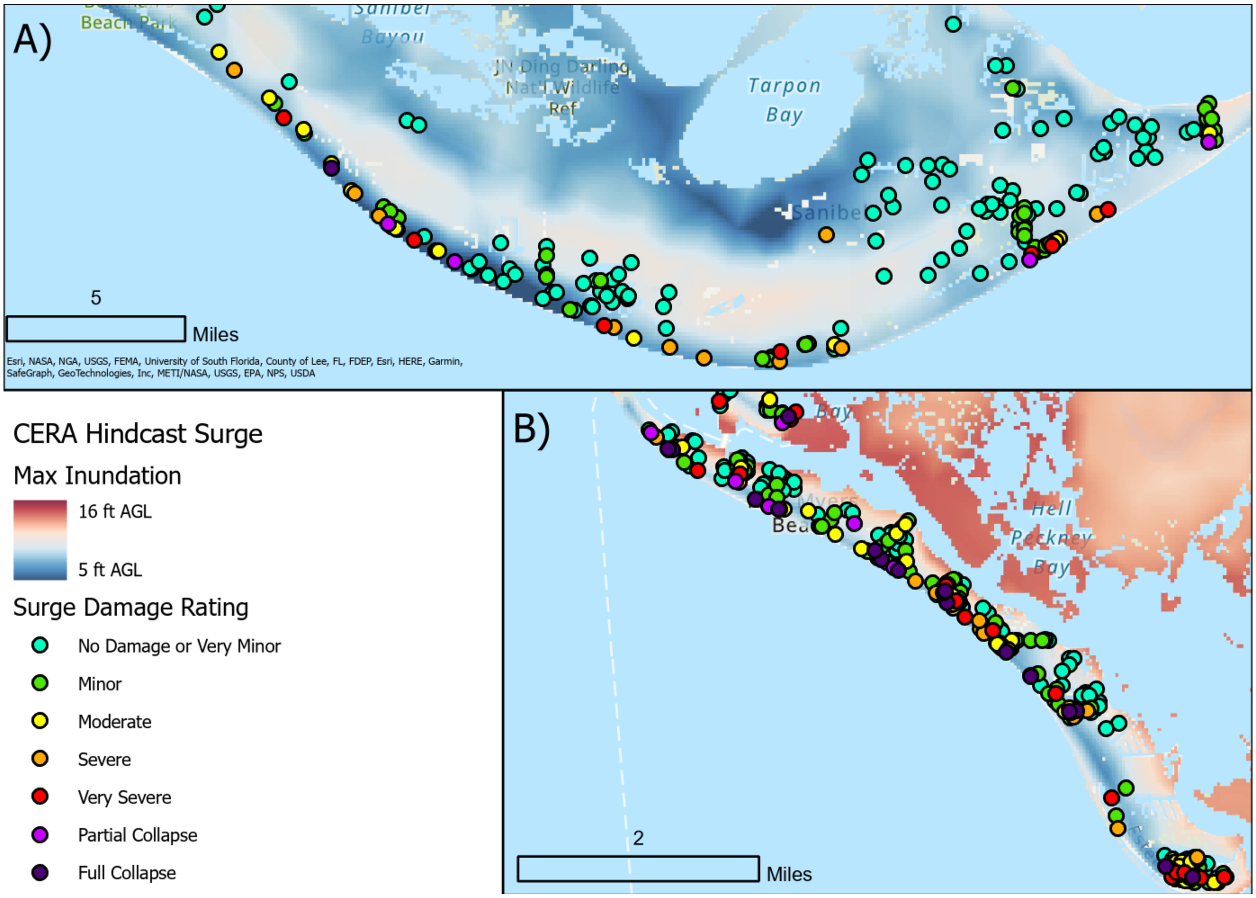

Figure 17. Spatial distribution of surge damage ratings in (A) Sanibel and (B) Fort Myers Beach.

The effect of construction era on the surge damage rating is stark. Of the structures constructed pre-FBC (2001 and prior), 20% experienced an SDR of 4 or higher (indicating some repairable structural damage up through complete collapse), while no post-FBC (2002 and later) structures experienced an SDR of 4 or higher. In essence, the damage to coastal structures constructed to the Florida Building Code subjected to historic storm surge levels was confined to damaged breakaway walls and minor damage to wall cladding induced by the failures of the breakaway walls. No significant exterior, surge-induced, structural damage was observed to the primary living area in any post-FBC homes in the study dataset. Interior damage was outside of the scope of this study.

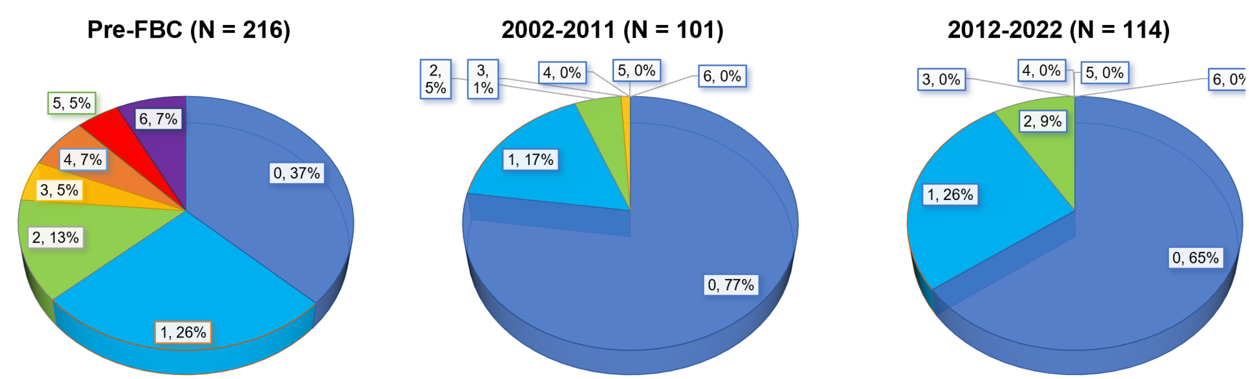

Figure 18. Distribution of surge damage ratings by construction era.

Some causal factors behind the enhanced vulnerability of pre-FBC structures are illustrated in Table 4. Specifically, 25% of the pre-FBC structures were located seaward of the Coastal Construction Control Line, meaning they were likely subjected to the worst wave impacts, compared to 17% of the 2002-2011 and 28% of the 2012-2022 structures. Pre-FBC structures also had an average elevation to Lowest Horizontal Structural Member of 4.8 ft relative to grade, compared to 7.6 ft for 2002-2011 structures, and 9.3 ft for 2012-2022 structures. In summary, pre-FBC structures were subjected to similar levels of hazards relative to the post-FBC structures, but lacked the elevation of the post-FBC structures. This likely explains much of the difference in performance, but construction practices and engineering design also likely play a role. As shown in Figure 19, the surge hazard level (as represented by the maximum surge inundation) was similar across pre-FBC and post-FBC structures. From the same figure, the surge hazard relative to the ELHSM is shown to be higher in pre-FBC structures than post-FBC, but nearly 20% of the post-FBC structures still had surge inundation estimated at higher than the ELHSM by 5 ft or more. The lack of structural damage to these structures suggests that engineering design and construction also played a significant role in mitigating damage beyond that of elevating the living area of the building. Figure 20 gives further evidence of this by showing that the mean damage rating increases with increasing inundation relative to the ELHSM. Within each category of inundation level, the higher surge damage is generally experienced by older structures.

In summary, the analysis shows that the flood regulations imposed by FEMA through the flood maps, and the structural design and construction regulations imposed by the Florida Residential Building Code, are in combination effective at preventing structural damage in compliant structures even during a historic storm surge event of the magnitude induced by Hurricane Ian.

Table 4. Surge performance of buildings subjected to surge hazards by construction era.

	Construction Era			
	Pre-FBC	**2002 - 2011**	**2012 - 2022**	**All**
No. Records	216	101	114	431
SDR = 0	37%	77%	65%	54%
SDR = 1	26%	17%	26%	24%
SDR = 2	13%	5%	9%	10%
SDR = 3	5%	1%	0%	3%
SDR = 4	6%	0%	0%	3%
SDR = 5	5%	0%	0%	2%
SDR = 6	7%	0%	0%	4%
Mean SDR	**1.6**	**0.3**	**0.4**	**1.0**
N_{CCCL}	55	17	32	104
Mean Surge (CERA), ft	8.9	9.0	9.1	9.0
Mean Surge (HWM), ft	7.9	6.8	9.1	8.0
Mean Elevation to LHSM, ft	4.8	7.6	9.3	6.6

Notes:
SDR = surge damage rating
N_{CCCL} = number of records seaward of the Coastal Construction Control Line
Mean Surge (CERA), ft = average estimated surge inundation above ground level in ft based on hindcast ADCIRC simulations sourced from CERA.

Mean Surge (HWM), ft = average surge inundation above ground level in ft based on linear interpolation between measured high-water marks collected by StEER and USGS.

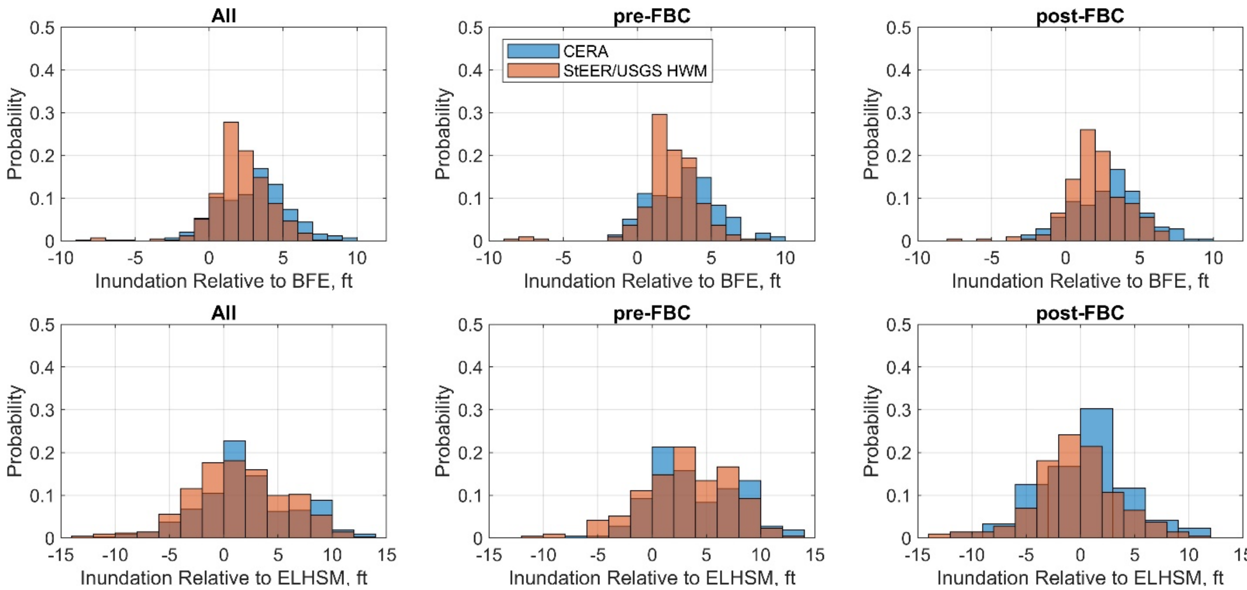

Figure 19. Surge inundation relative to the base flood elevation and estimated elevation to lowest horizontal structural member by construction era. Inundation is shown based on the CERA ADCIRC hindcast and interpolation of StEER and USGS HWM.

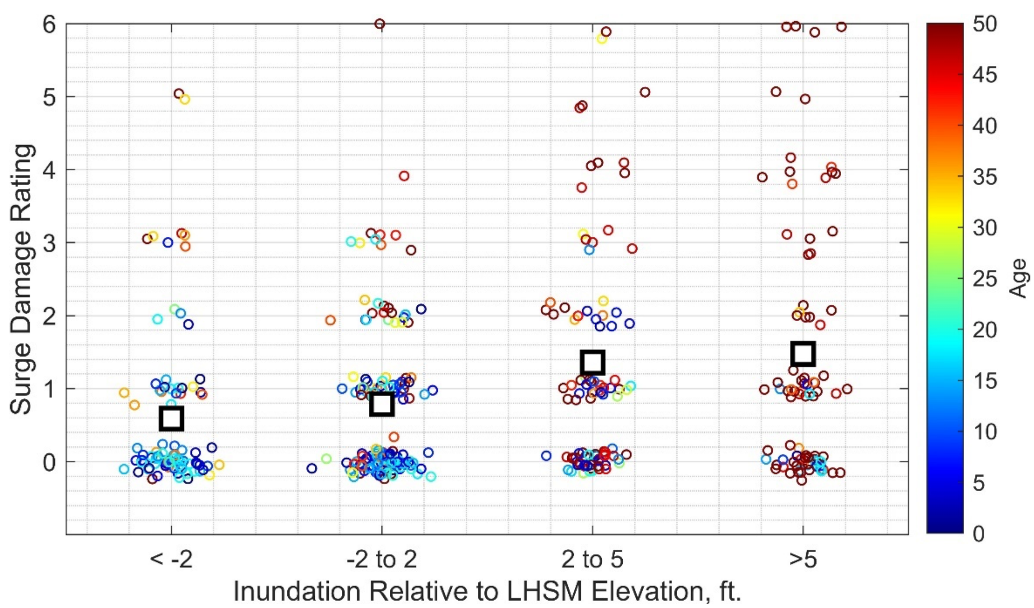

Figure 20. Surge damage ratings conditioned on the surge inundation (StEER/USGS high-water marks) relative to elevation of Lowest Horizontal Structural Member in feet. Random jitter has been added to points to aid interpretation, and markers are colored based on the age of the structure relative to 2022. White filled boxes are the mean surge damage rating.

5.2 Performance of Breakaway Walls

The performance of breakaway walls is stratified by the completeness of the failure, code era, and locality. Out of the study dataset, 278 residential structures were identified as most likely having breakaway walls either partially or fully enclosing the ground floor. These were reasonably distributed between pre-FBC, pre-2010 FBC, and post-2010 FBC construction eras as shown in Table 5. Independent of construction era, approximately 20% of structures with breakaway walls exhibited partial failure, meaning some portion (nominally more than 10%) of the enclosure area on the coastal-facing side of the structure remained intact while the remaining portion broke away. Some examples of partial breakaway wall failures in post-2010 FBC structures are provided in Figure 21. Additionally, there were multiple instances of the wall cladding (and in at least one case portions of the wall structure) immediately above failed breakaway walls that experienced damage. It was not possible to determine whether the damage to the walls above the breakaway walls was caused by improper attachment detailing of the breakaway walls, surge levels reaching above the top of the breakaway walls, or some other factor.

Considering locality, Ft. Myers Beach experienced over twice the percentage of breakaway wall failures (50% vs 23%) among homes that were classified as having breakaway walls. Hazard levels, based on the CERA hindcast surge inundation above ground level, were similar between the two localities with the homes on Ft. Myers Beach having an average modeled surge inundation of 8.2 ft (standard deviation of 3.9 ft) compared to 7.1 ft (standard deviation of 3.2 ft) for Sanibel.

Table 5. Frequency of complete and partial breakaway walls failures by construction era.

	Construction Era			
	Pre-2002	2002 – 2010	2011 - 2022	All
Breakaway Walls Present	83	77	108	278
Partial Failures	23 (28%)	11 (14%)	22 (20%)	62 (22%)
Complete Failures	43 (52%)	7 (9%)	15 (14%)	46 (17%)

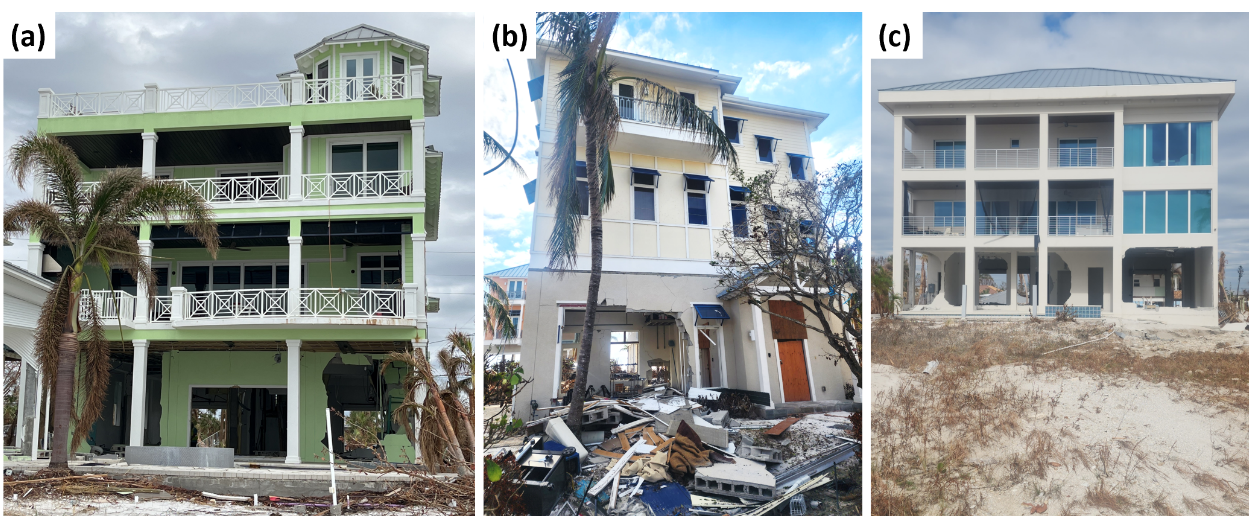

Figure 21. Examples of partial breakaway wall failures, including (a) a home on Ft. Myers Beach with CMU breakaway walls constructed in 2015; (b) a home on Ft. Myers Beach with CMU

breakaway walls constructed in 2015, and (c) a home on Ft. Myers Beach with CMU breakaway walls constructed in 2017.

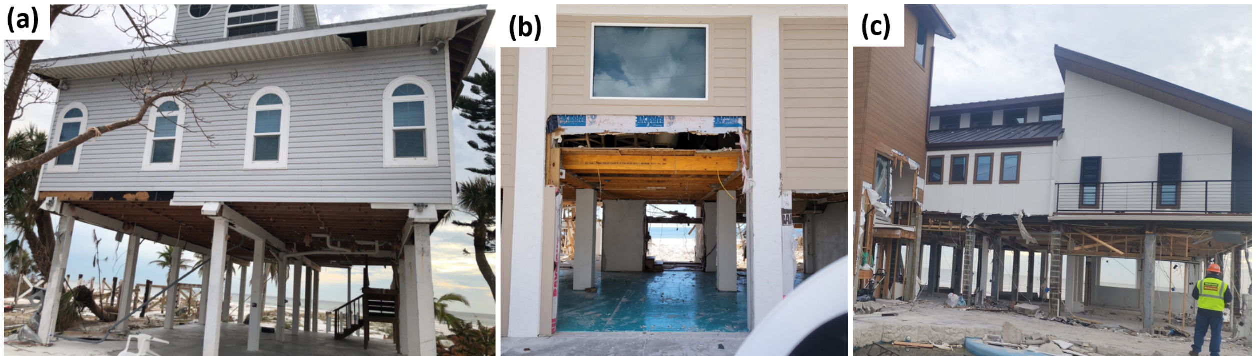

Figure 22. Examples of breakaway wall failure damaging wall cladding. (a) a home in Ft. Myers Beach constructed in 1991 with vinyl siding cladding; (b) a home in Ft. Myers Beach constructed in 1950 with fiber cement cladding; (c) a home in Ft. Myers Beach constructed in 1990 with composite wall panel cladding.

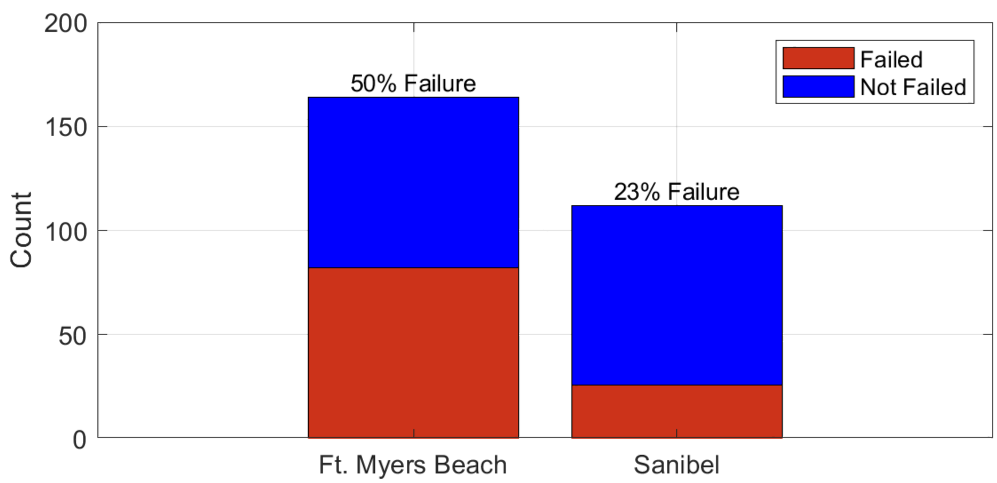

Figure 23. The proportion of breakaway wall failures (complete or partial failures) observed in Sanibel and Fortt Myers Beach among homes observed with breakaway walls.

5.3 Debris Impact Damming

Out of 431 structures that were assigned surge damage ratings in the study, 34 were identified as being likely affected by debris impact, but it was not feasible to ascertain whether debris impact damming specifically contributed to any failures. Sources of moving debris included breakaway walls from upstream structures, complete collapses of older, more vulnerable structures, and loose debris from storage and other sources. Figure 24 and Figure 25 show some examples of debris impacts.

Figure 24. Examples of debris impact damming on Fort Myers Beach that did not result in collapse of the impacted structures (GPS Location: 26.452799°, -81.952546°).

Figure 25. Before (left) and after (right) views of a cluster of homes affected by the impact of storm surge debris. To what extent debris damming contributed to the failures as opposed to the impact of moving debris could not be ascertained (GPS Location: 26.424844°, -81.906611°).

6 PERFORMANCE OF BUILDINGS SUBJECTED TO WIND HAZARDS

6.1 Overall Wind Performance

Hurricane Ian was far from a design-level event based on the wind field modeling performed by NIST/ARA, but wind damage[2] was still frequently observed in the study dataset as shown in Figure

[2] Separating between wind and surge damage is challenging, and thus component-level damage was defined independent of hazard source. Component-level damage was not assigned to breakaway walls. For analysis of wind damage, any structure with a surge damage rating of 3 or lower was excluded from the analysis.

27 and Figure 26. However, as illustrated in Table 6, nearly all the observable damage was related to the building envelope, specifically roof cover and wall cladding loss. Overall, 37% of buildings in the dataset were observed with damage to roof cover, and 13% of buildings were observed with wall cladding damage. Here it is assumed that all this damage is caused by wind, although it is possible that some of damage to both roof cover and wall cladding was induced by storm surge for some buildings on the barrier islands, primarily some located in the southern end of Fort Myers Beach, that saw inundation reach close to the eave height. Damage to the building envelope was most common in pre-FBC structures, but it was still commonly observed in post-FBC buildings (39% and 20% for construction eras of 2002-2011 and 2012-2022 respectively). While building envelope damage was common observed in approximately 5% of such structures), structural damage was uncommon even in pre-FBC structures, and no structural damage (roof or wall structure, roof or wall sheathing) was observed in post-FBC structures.

Wind damage was nominally correlated with the estimated gust wind speed (Figure 28), with increasing probability of exceeding roof cover damage limit states (e.g., 25% of roof cover loss). The enhanced probability in the lowest wind speed bin (80-100 mph) is possibly due to surge-induced damage in the southern portions of Fort Myers Beach, as inundation levels were close to or even greater than the eave heights of some slab-on-grade buildings.

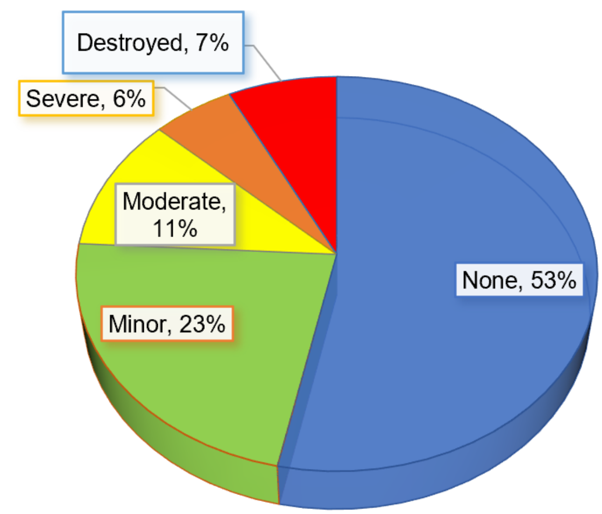

Figure 26. Distribution of wind damage ratings.

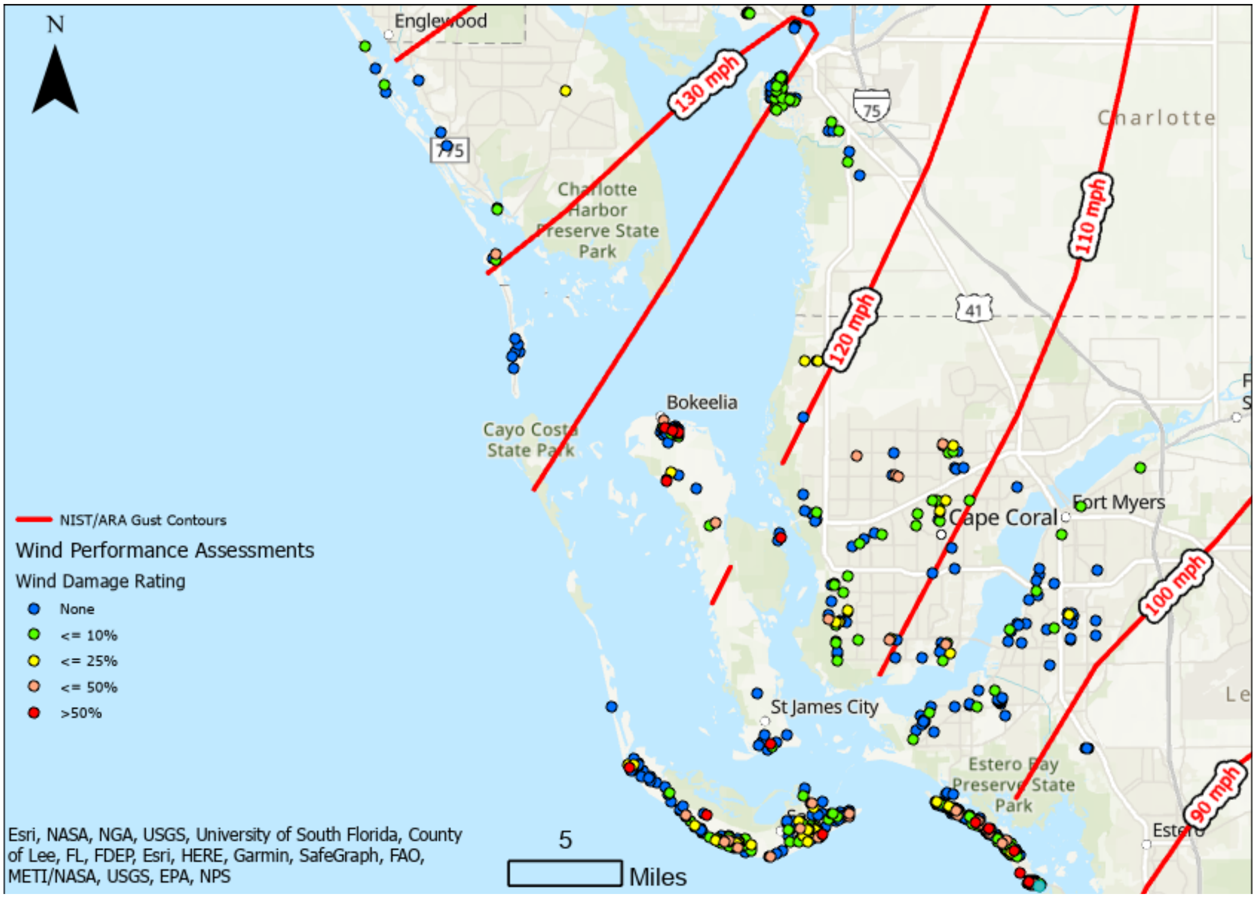

Figure 27. Spatial distribution of wind-induced roof damage relative to the Hurricane Ian best track and the estimated peak wind gust contours from NIST/ARA.

Table 6. Wind-induced roof damage occurrence by construction era and building component.

	Construction Era			
	Pre-FBC	**2002 - 2011**	**2012 - 2022**	**All**
No. Records	288	264	253	811
Any Roof Cover Damage	50%	39%	20%	37%
Any Roof Sheathing Damage	5%	0%	0%	2%
Any Roof Structure Damage	1%	0%	0%	0%
Any Wall Cladding Damage	19%	9%	11%	13%
Mean Gust WS, mph	109	111	110	110

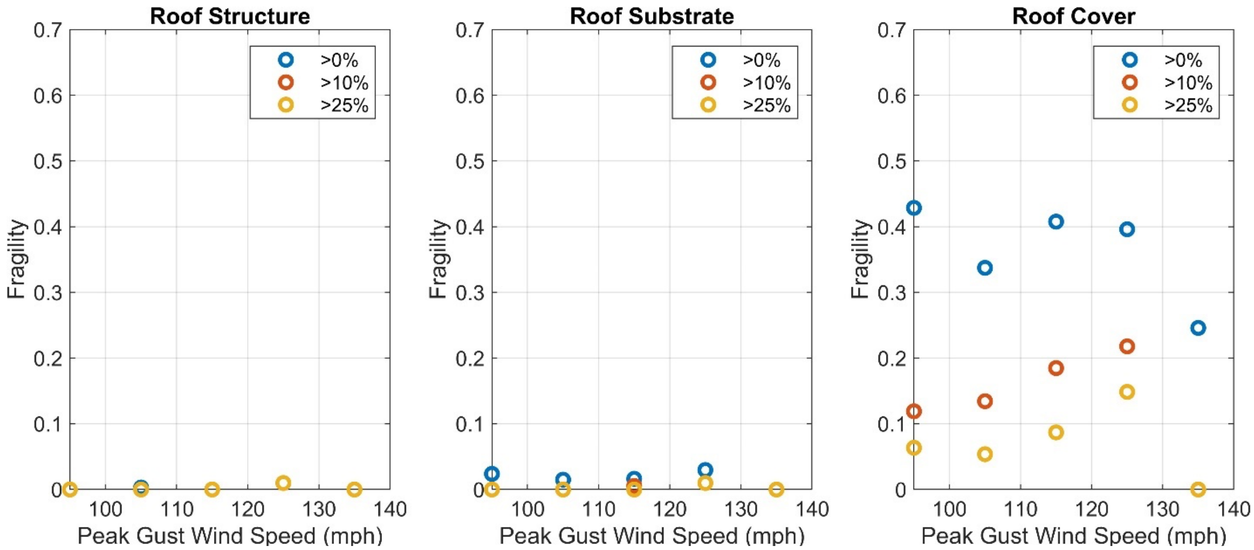

Figure 28. Probability of experiencing more than the specified component-level roof damage as a function of the estimated peak gust wind speed.

6.2 Roof Cover Performance

Since roof cover damage was commonly observed, a more detailed analysis was carried out to evaluate the performance of roof cover as a function of material and age of installation. The roof cover material was grouped into the following three main categories: (1) asphalt shingles, which included 3-tab and laminated asphalt-based shingles; (2) tiles, which included both concrete and clay tiles; and (3) metal, which included metal shingles, corrugated metal panels, and standing seam metal panels. In the roof material study dataset, metal roofs were most common (N = 338), followed by asphalt shingles (N = 221) and tile (N = 179). The age of the roof was obtained by taking the maximum of the year of construction of the base structure and the year of the latest roof permit (if present). Out of the 768 roofs, 189 had roof permits on file that were fulfilled prior to Hurricane Ian.

The results of the analysis show that for all roof cover materials, damage is rare within the first five years of installation (Figure 29). Metal and tile roofs show negligible increase in damage with age until the roof is greater than 10 years old. In contrast, asphalt shingles show a significant increase in average damage after just 5 years of service life. From a different perspective, beyond 5 years of service life, almost 50% of asphalt shingle roofs had at least 5% of visible damage, compared to around 10-15% for tile and metal roofs. This damage may be repairable but emphasizes the importance of effective secondary water barriers to minimize economic impacts of such damage. It should be noted that for roof ages beyond 20 years, the roof age is more uncertain as permit records do not go back that far on the county websites.

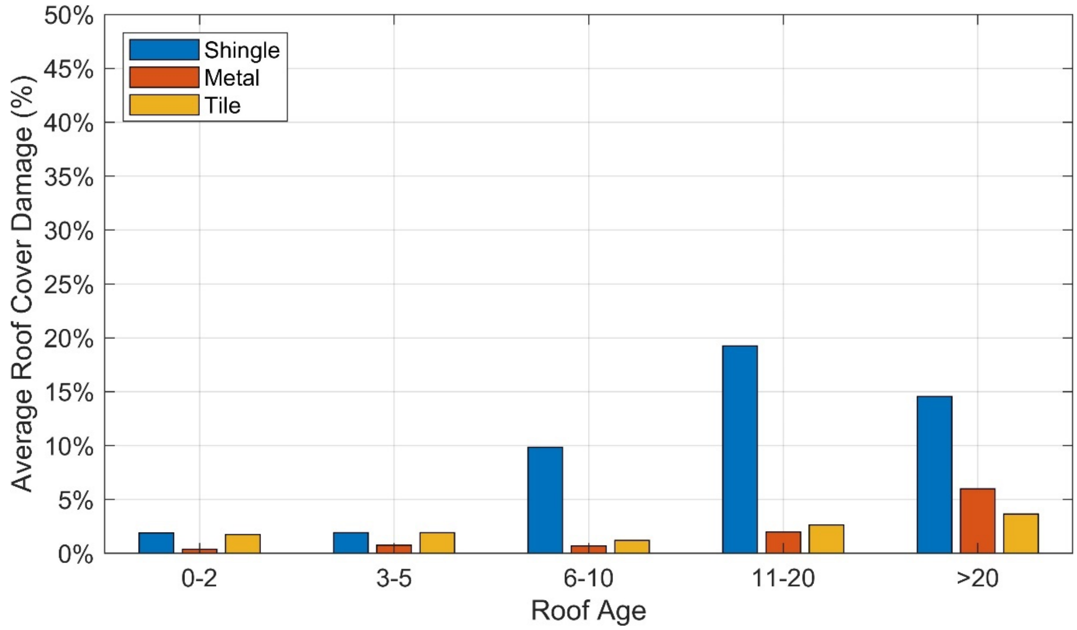

Figure 29. Average roof cover damage by roof cover material classification and age of the roof, obtained from building permits and county records.

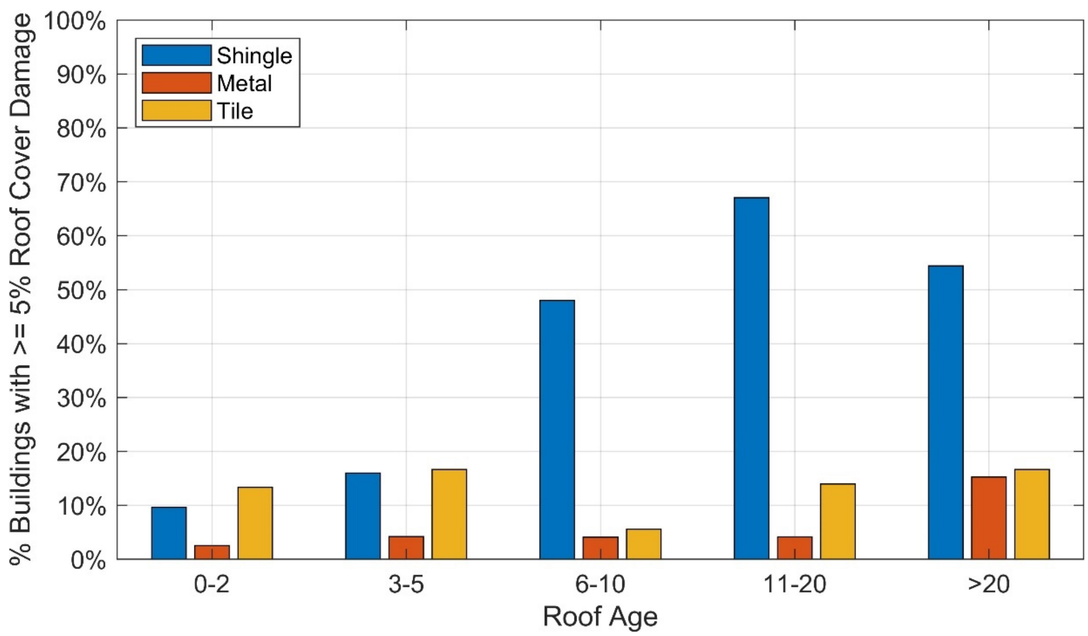

Figure 30. Percentage of buildings with at least 5% visible roof cover loss by material and roof age.

6.3 Wall Cladding Performance

Wall cladding materials are more varied than roof cover materials, and so grouping into common types is challenging. For comparison however, separate groups were created for vinyl siding, fiber cement boards, composite materials, and other. Most of the buildings in the study dataset (N = 405) were identified as having stucco as the building exterior, typically indicative of a concrete or masonry structural system. Of the other materials, vinyl siding (N = 96), fiber cement boards (N = 124), and composite panels (N = 87) were the most used based on the study observations. Many homes used multiple cladding types, with one dominant material and one secondary material.

Regarding performance (Figure 31), a few recently built homes with fiber cement boards experienced minor wind damage, but most wall cladding in service for 5 years or less performed well in terms of visible exterior damage. It should be noted that there were no vinyl siding systems installed within the past two years in the study dataset. Some older (> 20 years old) vinyl siding systems experienced more significant damage, but these would have been installed pre-FBC if the age of the wall cladding matches the original year of construction of the material. As illustrated further in Figure 32, the wall cladding damage that does occur is generally minor. Less than 20% of buildings regardless of wall cladding system and age experienced more than 10% wall cladding loss.

In summary, wall cladding systems generally performed reasonably overall, but should be understood within the context of the estimated wind hazard, which was well below design levels. In a design level event, wall cladding damage would be much more widespread, even in post-FBC buildings, based on the observations from this study dataset.

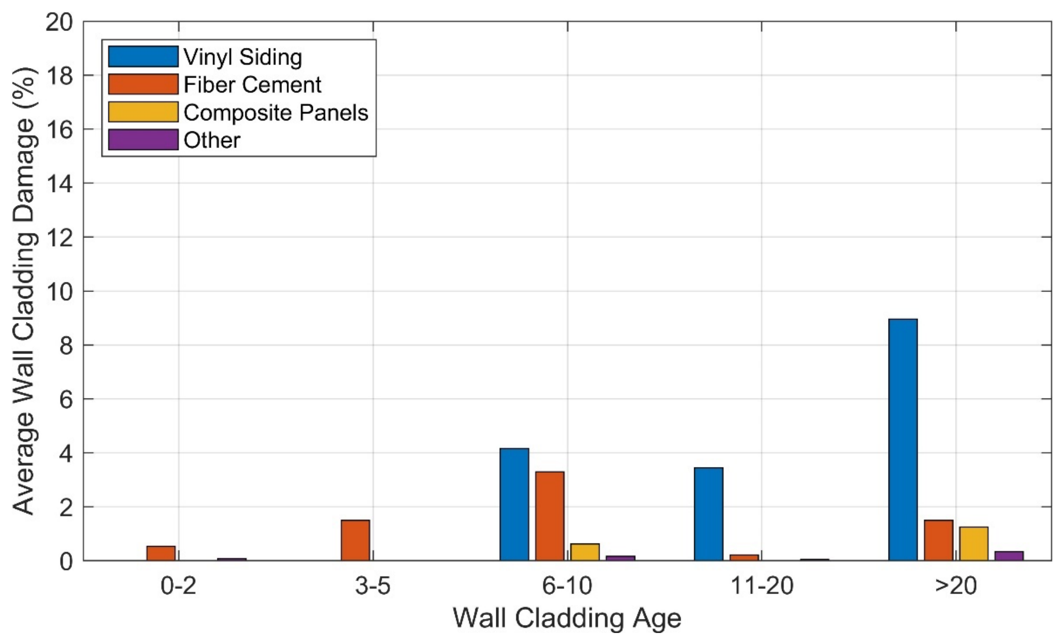

Figure 31. Average wall cladding damage by material classification and age (in years) of the building.

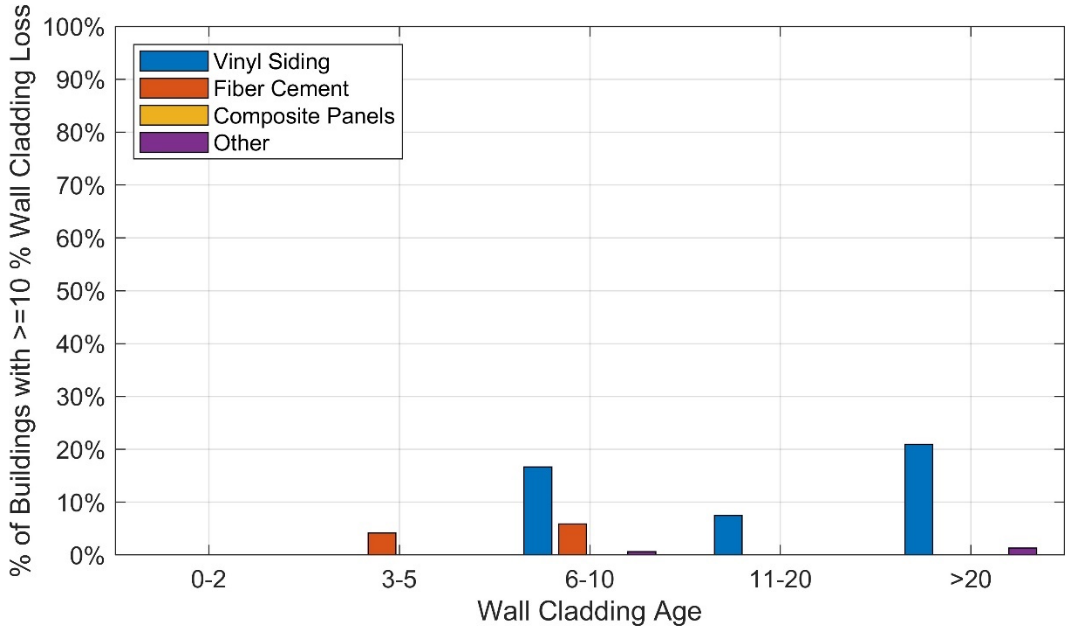

Figure 32. Percentage of buildings with at least 10% visible wall cladding loss by material and age of original construction (in years).

6.4 Performance of Sunrooms

Sunrooms are governed by Section 301.2.1.1.1 of the 2020 Florida Residential Code, which in turn references AAMA/NPEA/NSA 2100 for more detailed design specifications. Sunrooms are to be treated as Risk Category I structures, and enclosures must be able to resist Main Wind Force Resisting System pressures and Components and Cladding pressures as per ASCE 7. In the regions affected by Hurricane Ian, Category I basic wind speeds vary between 140-150 mph, compared to approximately 150-160 mph for Risk Category II structures.

Out of 233 homes in the Hurricane Ian study dataset that were identified as having sunrooms, 74 (or 30%) were identified as being visibly damaged, with most of these partially or fully collapsed, and others experiencing only damage to screen panels. Most of these sunrooms were Category I per the Florida Building Code, meaning they were covered outdoor spaces with insect screening enclosures. The average estimated 3-second gust wind speed associated with the sunroom locations was 113 mph, approximately 75% of design levels, but 52 of the damaged sunrooms were observed on Ft. Myers Beach or Sanibel, where storm surge likely contributed to the damage. Frequently, the debris from the sunrooms was scattered, potentially causing damage to the main building structure or neighboring buildings. The year in which the sunrooms were manufactured or installed was outside of the scope of the study, but a few were collected for illustrative purposes (Figure 33 and Figure 34).

Figure 33. Illustrative post-Ian view of sunroom performance in Cape Coral, FL. Out of the three visible sunrooms, one collapsed. The collapsed sunroom was built in 1999, while the other two were constructed in 2007 and 2018.

Figure 34. Examples of sunroom performance on Sanibel Island, including (A) collapse of a sunroom constructed in 2007, and (B) partial removal of the screen panels in a sunroom constructed in 2007. Sunrooms on the barrier islands would have been subjected to both high winds and storm surge in most locations.

6.5 Performance of Solar Systems

Solar systems have become increasingly popular in the Sunshine State, including rooftop solar photovoltaic panels and solar hot-water systems. As part of the DEQC efforts of this project, the performance of rooftop solar systems (which included solar hot-water systems) was quantified on the sample of structures within the scope of this project. Out of 54 roofs in the study dataset identified as having rooftop solar systems, 30% were identified as being partially or completely removed off the roof. Figure 35 shows some examples of failed rooftop solar systems. The average estimated 3-second gust wind speed experienced by the damaged solar systems was 105 mph, well below design levels.

Per Section R324.4.1.2 of the Florida Residential Code, roof mounted solar panels must be designed and installed to resist wind loads in accordance with ASCE 7. Prior to ASCE 7-16, the wind load provisions did not provide direct wind load criteria for rooftop solar panels, and so wind loads were based on ASCE 7 Chapter 30 Components and Cladding. Specific load provisions for solar panels were added in ASCE 7-16, which was first adopted in the 2020 version of the Florida Residential Code, which was effective December 31, 2020. All the damaged rooftop solar systems observed in this sample study were installed prior to 2021.

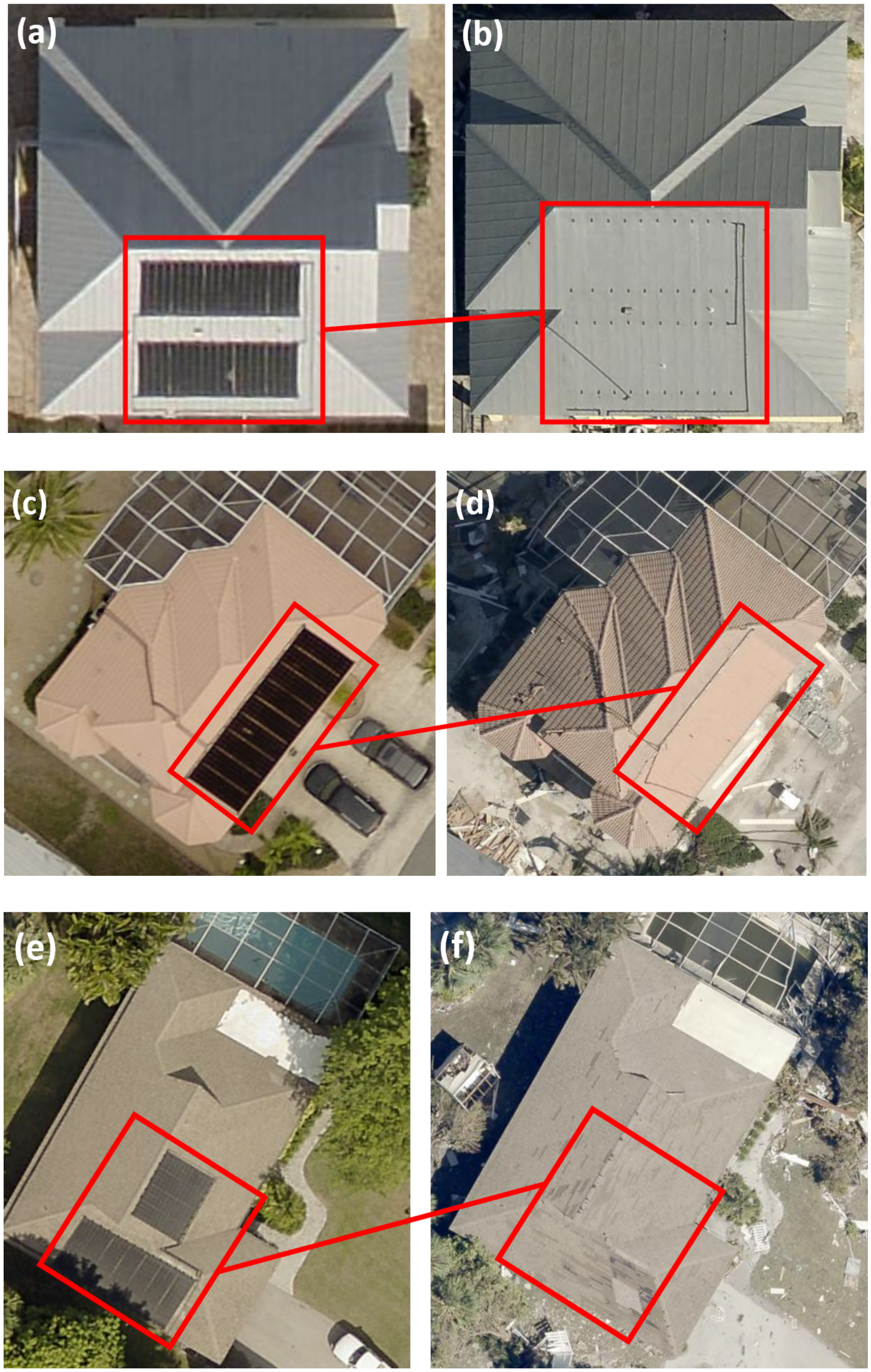

Figure 35. Examples of rooftop solar system performance, each including pre- and post-Ian aerial views sourced from Pictometry EagleView; (a,b) two-story home on Ft. Myers Beach with a rooftop solar system installed in 2012; (c,d) one-story home on Ft. Myers Beach with a rooftop solar system installed in 1997; and (e,f) one-story home on Ft. Myers Beach with a rooftop solar system installed in 2020.

7 CONCLUSIONS

Hurricane Ian subjected the central west coast of Florida between Fort Myers and Port Charlotte to historic storm surge in combination with high winds. The storm surge caused catastrophic damage to communities on Fort Myers Beach, Sanibel, San Carlos island, and more. While the wind damage was less severe, widespread damage to the building envelope was observed, even in post-FBC structures, despite estimated gust wind speeds being less than 70% of current design levels. From the results of this study, the following conclusions are made.

7.1 Conclusions Relevant to the Florida Building Code

1. Residential buildings constructed to the 2002 Florida Building Code or later suffered minimal observable, structural damage from either wind or surge hazards. The lack of wind damage is expected, given that the estimated wind speeds were well below design. The lack of surge damage appears to be attributable to (1) appropriate elevation of the main living areas to at least the base flood elevation as defined by the FEMA FIRMs, and (2) enhanced construction requirements for lateral loads in the Florida Building Code Residential.
2. Breakaway walls observed in the study dataset mostly performed as intended. Although examples of partial failures were observed, they did not lead to any observed structural failures in the foundation in post-FBC structures. It is possible that improper breakaway wall performance contributed to the collapse of some pre-FBC structures that were completely washed away, but any evidence to this effect would have been washed away with the structures.
3. This study did not find evidence that structures built to the Florida Building Code seaward of the Coastal Construction Control Line (CCCL) performed worse than those located inland of the CCCL.
4. Structures on Sanibel were less likely to experience severe surge-induced damage relative to those on Fort Myers Beach, despite similar high-water mark elevations being recorded on the two islands, and similar proportions of structures constructed pre- and post-FBC. Potential reasons are the higher coverage of vegetation (e.g., trees, shrubs) on Sanibel relative to Fort Myers Beach. The authors suspect that building setback distance, and even directional orientation of the islands may contribute as well but further study is warranted.
5. Roof cover systems of all kinds installed within the last 5 years performed well under Hurricane Ian's winds, but their vulnerability increases with age. To what extent the better performance of recently installed systems is due to improved products or installation vs lack of aging/degradation is unclear. Asphalt shingles exhibited markedly worse performance after 5 years than other roofing systems, with nearly 50% of buildings in the study dataset experiencing loss of at least 5% of the roof cover system. The effects of aging were less pronounced in metal and tile roofs, but both systems consistently exhibited less vulnerability to wind than asphalt shingle systems.
6. Wall cladding systems generally experienced less damage than roof cover but was still observed in 13% of the structures in the study dataset, with nearly twice the frequency of occurrence in pre-FBC homes relative to post-FBC homes. Vinyl siding and fiber cement board systems were the most frequently damaged.
7. Appurtenant systems, such as rooftop solar panel systems and sunrooms, were frequently damaged by wind despite the relatively low wind speeds with respect to design levels. Approximately 30% of rooftop solar systems were partially or completely removed from

the roof, and a similar percentage of sunrooms experienced full or partial collapse. Indirect effects of these damages were not quantified in this study.

7.2 Recommendations Relevant to Follow-Up Studies on Building Performance

1. This study does not evaluate the performance of structures with respect to wind-driven rain, rainwater ingress, and interior damage due to storm surge. Such effects are potentially severe even in many of the structures having no visible exterior damage as identified in this study as. Previous studies have used follow-up interviews with residents, which currently remains the best method for quantifying these effects.
2. Anecdotally, several roofs with secondary water barriers appeared to have experienced loss of the secondary water barrier, exposing the bare deck to rainwater ingress. While this was outside the scope of the current project, a dedicated study on this issue may be needed, related to item (1) above.
3. The relatively high frequency of damage to rooftop solar systems and sunrooms in a well below design event warrants further forensic investigations to identify more precisely the type of system, dates of installation, causes of failure, and indirect damage caused if any.
4. Engagement of the public and community leaders is needed to obtain their perspective on the performance of code-compliant structures during Hurricane Ian. While overall, performance relative to both wind and surge hazards appears successful, it is unclear whether the general public agrees with this assessment of performance or understands what performance should be expected from code-compliant construction in below- and at-design hurricane events.

8 ACKNOWLEDGEMENTS

The efforts and dedication of the following data librarians who performed the Data Enhancement and Quality Control tasks is gratefully acknowledged: Hunter Desmond (Auburn University), Blake DiSalvo (Auburn University), Katie Hayden (Auburn University), Steven Klepac (Graduate, University of Florida), Catherine Klop (Auburn University), Maryam Klop (Auburn University), Sarah Prince (Auburn University), Rebecca Turochy (Auburn University), and Selena Zheng (Auburn University). The efforts of Graduate Research Assistants Jordan Nakayama (Auburn University), and Brandon Rittelmeyer (Auburn University) are also gratefully acknowledged.

9 REFERENCES

Alam, M. S., T. Kijewski-Correa, D. B. Roueche, I. Robertson, A. Safiey, K. M. Mosalam, P. Lynett, and J. Kaihatu. n.d. "Hurricane Ian's Impact on the Barrier Islands in Florida: Field Observations from the Coastal and Structural Damage Assessment Survey." *Prog.*

ARA. 2022. *Hurricane Ian Landfall in FL Peak Gust Wind Speeds (Release 3)*. Applied Research Associates.

Berman, J. W., J. Wartman, M. Olsen, J. L. Irish, S. B. Miles, T. Tanner, K. Gurley, L. Lowes, A. Bostrom, J. Dafni, M. Grilliot, A. Lyda, and J. Peltier. 2020. "Natural Hazards Reconnaissance With the NHERI RAPID Facility." *Front. Built Environ.*, 6.

Bucci, L., L. Alaka, A. Hagen, S. Delgado, and J. Beven. 2023. *National Hurricane Center Tropical Cyclone Report: Hurricane Ian (AL092022)*. Miami, FL: National Hurricane Center.

Cortes, M., P. Arora, L. Ceferino, H. Ibrahim, D. Istrati, D. Reed, D. Roueche, A. Safiey, T. Tomiczek, I. Zisis, M. Alam, T. Kijewski-Correa, D. Prevatt, and I. Robertson. 2022. "StEER: Hurricane Ian Preliminary Virtual Reconnaissance Report (PVRR)." Designsafe-CI.

Dubrow, A. 2020. "Frontera on the Front Lines During Record Hurricane Season." Accessed June 12, 2023. http://tacc.utexas.edu/news/latest-news/2020/10/13/frontera-front-lines-during-record-hurricane-season/.

FMEC. 2022. "Florida Medical Examiners Commission Hurricane Ian deaths."

Kijewski-Correa, T., D. Prevatt, D. Roueche, I. Robertson, M. Alam, A. Safiey, I. Zisis, O. Lafontaine, O. Nofal, L. Rhode-Barbarigos, A. Subgranon, D. Faraone, J. Micali, J. X. Santiago-Hernández, and D. Agdas. 2023. "StEER: Hurricane Ian Early Access Reconnaissance Report (EARR)." Designsafe-CI.

Kijewski-Correa, T., D. B. Roueche, K. M. Mosalam, D. O. Prevatt, and I. Robertson. 2021. "StEER: A Community-Centered Approach to Assessing the Performance of the Built Environment after Natural Hazard Events." *Front. Built Environ.*, 79. Frontiers.

Prevatt, D. O., and D. B. Roueche. 2019. *Evaluation of Wind Resistance of Vinyl Siding and Soffit Systems, and Performance During the 2017 Hurricane Irma*. 1–90. University of Florida.

USGS. 2022. "Hurricane Ian (2022) Flood Event Viewer." Accessed June 12, 2023. https://stn.wim.usgs.gov/FEV/#2022Ian.

Wickham, J., C. Homer, J. Vogelmann, A. McKerrow, R. Mueller, N. Herold, and J. Coulston. 2014. "The Multi-Resolution Land Characteristics (MRLC) Consortium — 20 Years of Development and Integration of USA National Land Cover Data." *Remote Sens.*, 6 (8): 7424–7441. https://doi.org/10.3390/rs6087424.

APPENDIX A. SUMMARY OF FCMP TOWER DEPLOYMENTS IN ADVANCE OF HURRICANE IAN (2022)

Deployment Dates
Monday, September 26, 2022 to Thursday, September 29, 2022

Travelers

- Alex Esposito
- Chris Ferraro
- Wyatt Kelch
- Forrest Masters
- Ryan Mieras
- Mesa Nicholas
- Benjamin O'Hern
- Brian Phillips
- Scott Powell
- Taylor Rawlinson
- Ian Van Voris

Tower T1

Punta Gorda Airport, Punta Gorda, FL
Latitude: 26.92786
Longitude: -81.99188
https://goo.gl/maps/JQvsZPZosXvSz73z6

10-m RM Young Wind Monitor, sampled at 10 Hz

- Max instantaneous wind speed: 53.2 m/s
- Max 3-sec moving average wind speed: 49.6 m/s
- Max 1-m moving average wind speed: 40.0 m/s

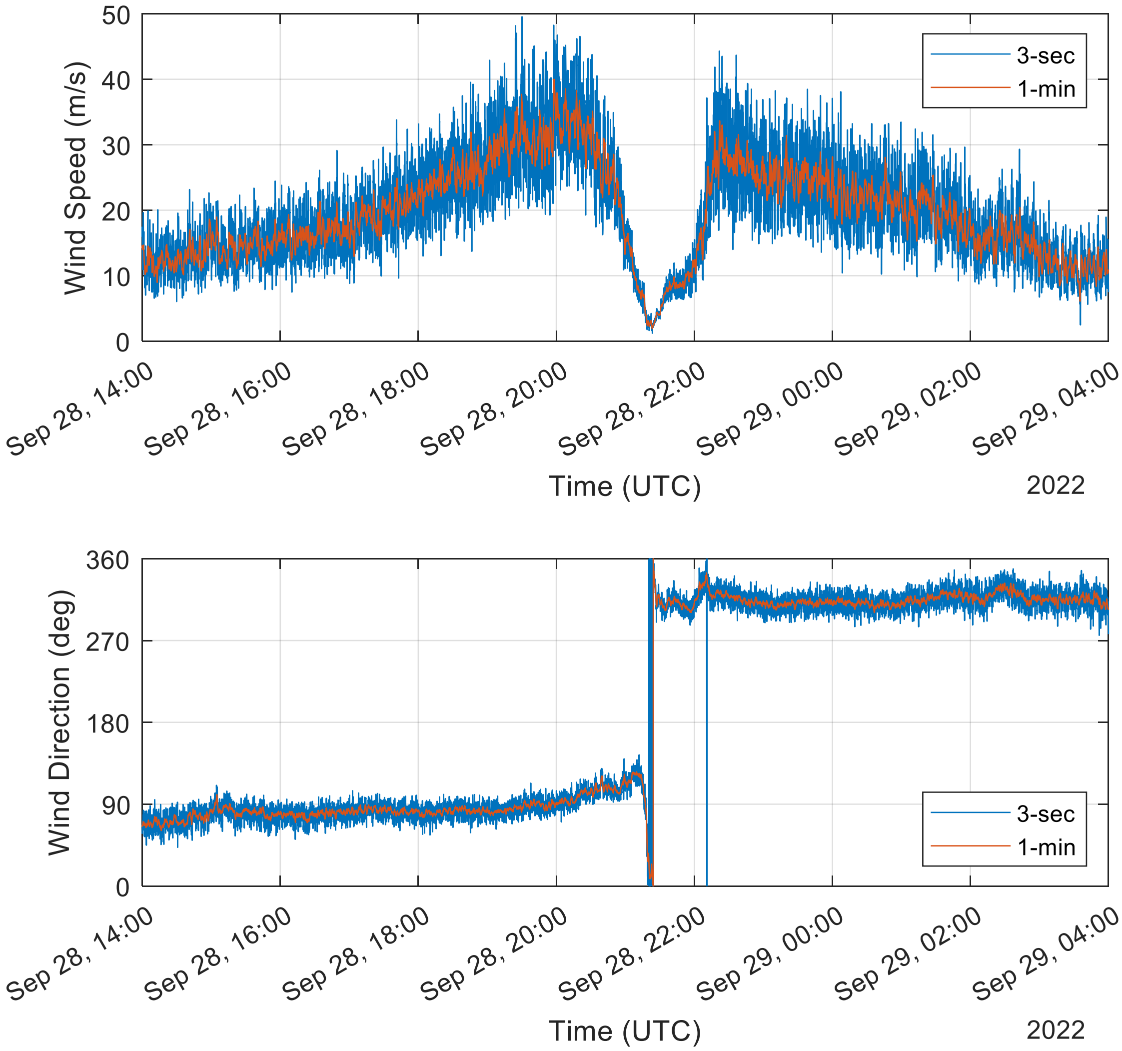

Figure A1. Wind speed and direction measured by FCMP T1.

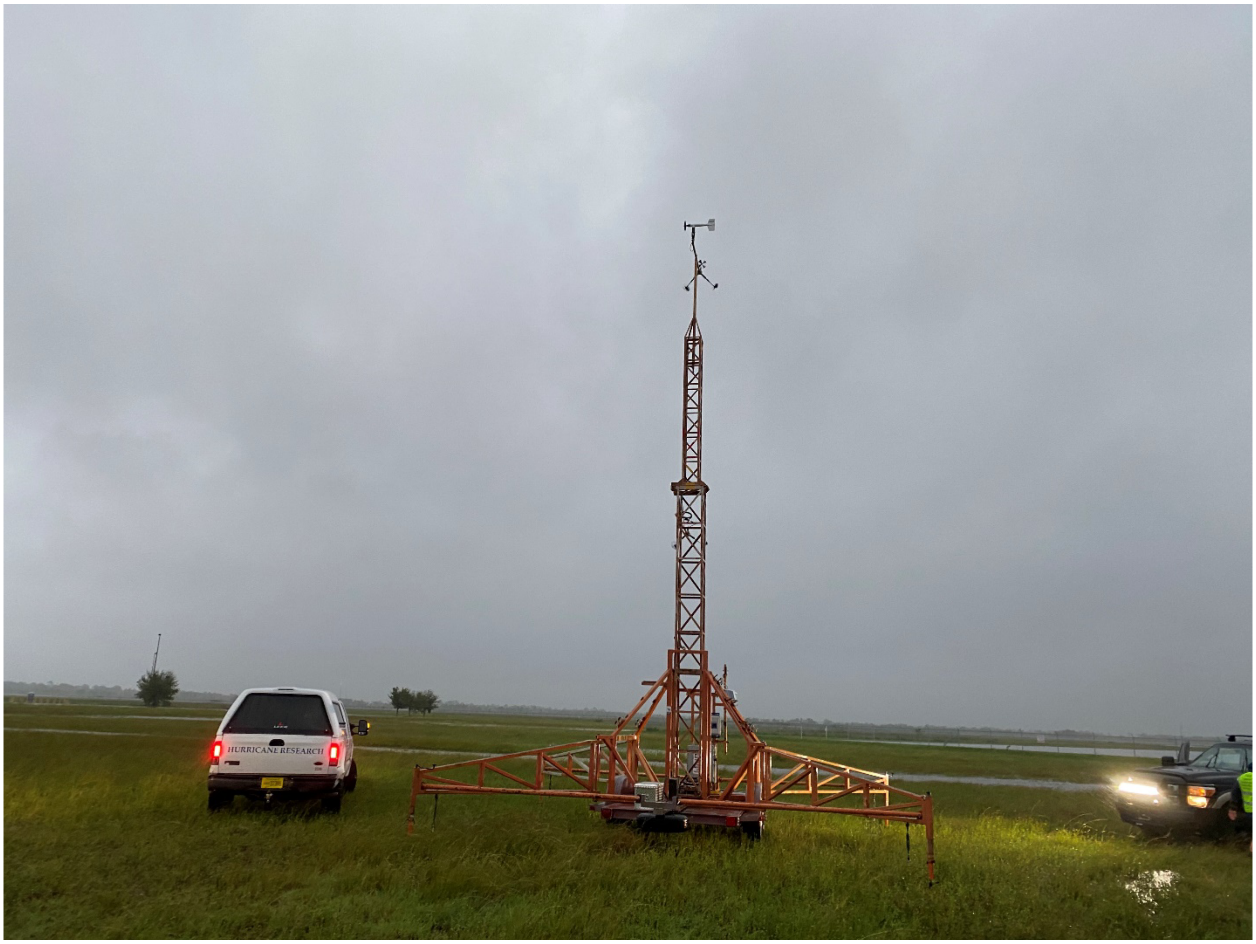

Figure A2. Siting of FCMP T1.

Tower T2

US HWY 41, Punta Gorda, FL
Latitude: 26.89584
Longitude: -82.02796
https://goo.gl/maps/KvJs6SQApVBz2sCv7

15-m RM Young Wind Monitor data, sampled at 10 Hz

- Max instantaneous wind speed: 54.5 m/s
- Max 3-sec moving average wind speed: 50.6 m/s
- Max 1-m moving average wind speed: 36.7 m/s

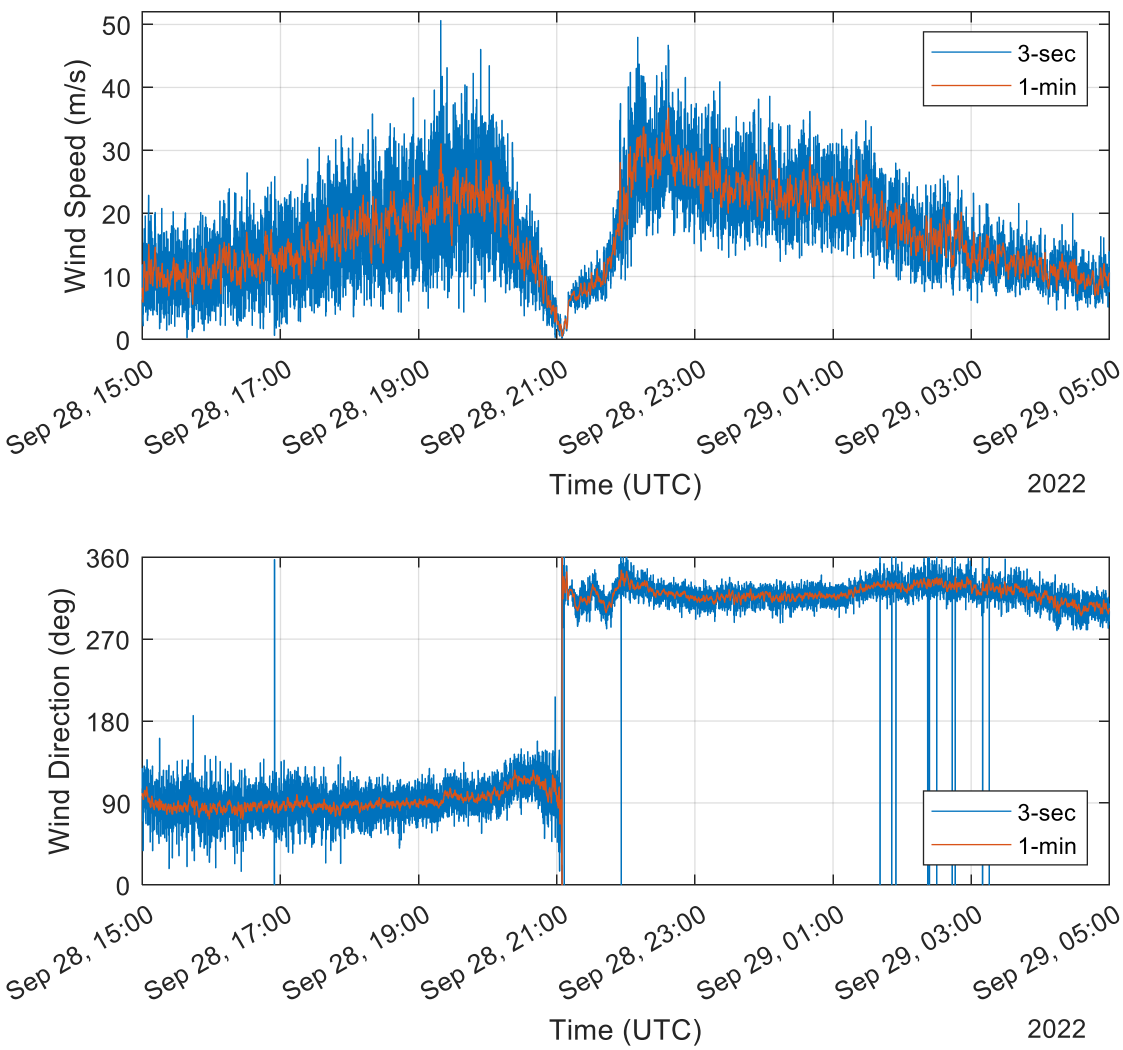

Figure A3. Wind speed and direction measured by T2.


Figure A4. Siting of FCMP T2.

APPENDIX B. SUMMARY OBSERVATIONS OF BUILDING PERFORMANCE DURING HURRICANE IAN (2022)

The following content is taken from the StEER EARR (Kijewski-Correa et al. 2023), which both PIs Prevatt and Roueche contributed to in authorship and editorial capacities. Metadata for the figures included in this section, including the source of the image and GPS locations, is provided at the end of this appendix.

Observed Performance

The following observations are listed based on preliminary review of the FAST-1 imaging, supplemented by the year built and other relevant information from public sources as needed. The area impacted by Hurricane Ian is broken down into three regions - the Barrier Islands near landfall, coastal urban regions, and inland regions. The primary focus herein is on the barrier islands and the coastal urban regions. Pictures taken during windshield assessments by FAST teams are included to support the discussion in each section, along with pre-storm imagery from the Google Maps platform and post-storm aerial imagery from NOAA where needed to provide context. Precise locations and imagery sources for all photos are provided in the Appendix. Note this complements the Media Repository compiled by the Virtual Assessment Structural Teams (VAST) and published under this same project: PRJ-3709 (Cortes et al. 2022).

4.1. Barrier Islands near Landfall (Sanibel, Pine Island, Fort Myers Beach, Bonita Beach)

The barrier islands bore the brunt of both the storm surge and high winds of Hurricane Ian; however, the hazards were not uniform. Estero Island (containing Ft. Myers Beach), Bonita Springs Beach, San Carlos Island, and Sanibel Island experienced the highest storm surge and wave impacts, but peak wind gusts were estimated to be between 100-110 mph (ARA, 2022). In contrast, barrier islands north of the track, such as Pine Island, Boca Grande, and Don Pedro Island, experienced minimal storm surge but were estimated to have experienced the highest wind gusts - between 120 and 130 mph. FAST-1 was able to document representative performance of structures throughout the barrier islands, and from a preliminary review of the imagery the following themes emerge:

- **The most widespread damage by far occurred in Ft. Myers Beach and was primarily tied to storm surge and wave action.** A hazard gradient was obvious in the damage patterns, with the regions with the expected strongest wave impacts near and coastward of the Coastal Construction Control line (roughly aligned with Estero Blvd in Ft. Myers Beach) correlating with the highest frequency of complete destruction. Destruction appeared to be correlated with freeboard elevation, as illustrated in Figure 4.1.

- **Coastal structures on Sanibel Island performed noticeably better from a structural perspective than those on Ft. Myers Beach,** with no observed examples of complete collapse or washout of structures except for a few buildings at the Sanibel Lighthouse. The improved performance is notable given that high water marks reported at the time of data collection are very similar between the two islands (Cortes et al., 2022). Potential causal factors for the improved performance are: (1) the greater setback of coastal buildings on Sanibel relative to Ft. Myers Beach (roughly 400 ft vs 200 ft, respectively), and (2) the abundance of vegetative features between the buildings and the coast in Sanibel Island which could have resulted in dissipation of much of the wave energy. Figure 4.2 shows a typical coastal building on Sanibel. Differences in building stock or construction practices also could be a factor. The median year of construction was 1981 for both Sanibel Island and Ft. Myers Beach / Estero Island, but construction practices may still differ between what are two distinct communities.

- **Breakaway walls appeared to perform as intended in most cases,** but it should be noted that a survivability bias is potentially present, since structures with breakaway walls that didn't perform as intended may have washed away, destroying evidence. Further study is needed. A couple examples of breakaway wall performance are illustrated in Figure 4.3.

- **In addition to direct lateral hydrodynamic loading on structures the storm surge and waves in Ft. Myers Beach produced a number of other effects** including sinkhole formation, significant scouring around piles and other structural members, and uplift of slabs and floor systems. Figure 4.4 illustrates some of these effects.

- **Critical facilities, as a whole, performed acceptably on the barrier islands,** based on what could be observed from the surface-level panoramas (illustrated in Fig. 4.5). One possible exception was the Ft. Myers Beach Fire Department District Station 31,which experienced partial wall collapse due to storm surge. This district station was constructed on grade, and approximately 500 ft from the coastline. Otherwise, from a structural perspective, both wind and storm surge performance appeared to be good. More in-depth assessments would be needed to evaluate functionality and other performance goals of these facilities.

- **Structural wind damage was rare in site-built structures,** even north of the track where peak wind estimates were highest, but there were isolated examples of structural roof failures and partial wall collapses in older residential buildings built prior to the adoption of the Florida Building Code in 2002 (Fig. 4.6).

- **RV and mobile/manufactured home parks exhibited poor performance under direct wave action, and were more likely to experience wind damage than site-built structures.** Under direct wave action, homes and parks were completely washed away (Fig. 4.7). Away from the coastline, several instances of homes pushed off of their unreinforced masonry pier foundations were observed due to storm surge or inland flooding, and wind damage was frequently observed, up to and including loss of the roof structure. The majority of the mobile/manufactured homes with wind damage observed in the preliminary review of the surface-level panoramas only experienced damage to the building envelope.

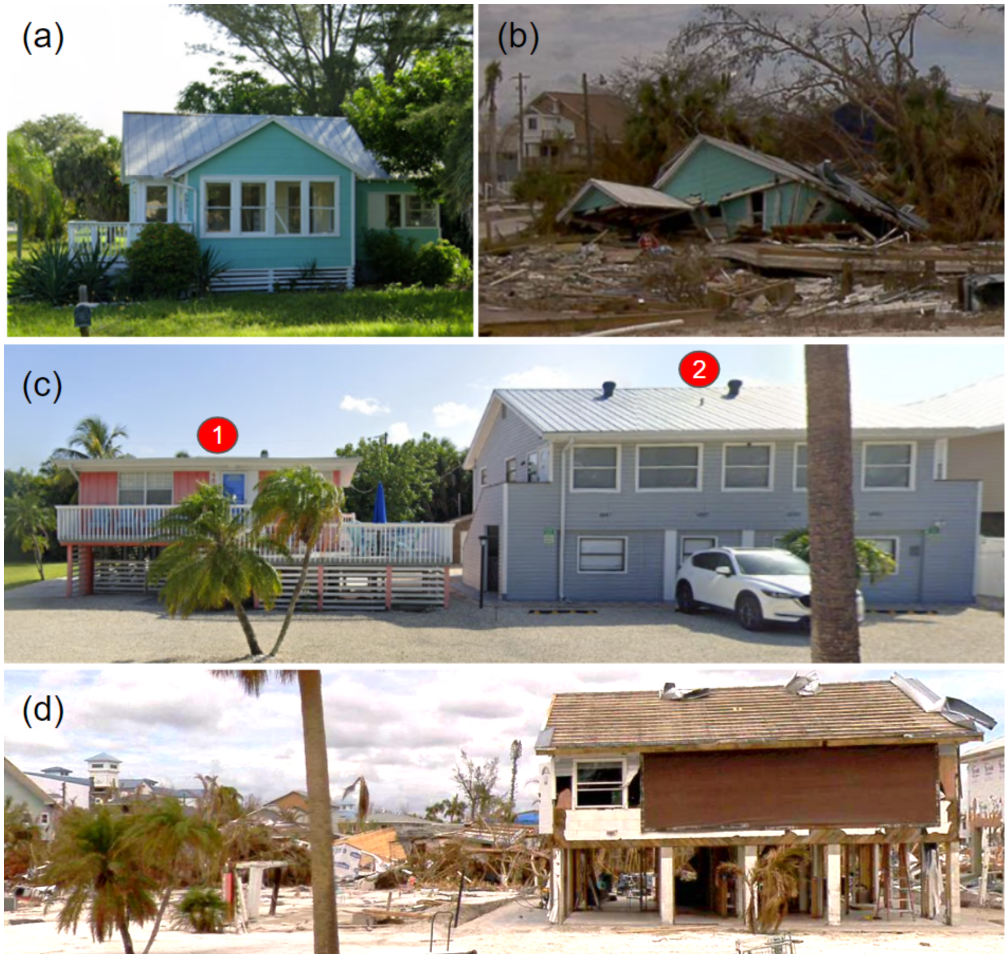

Figure 4.1. Importance of freeboard elevation to survivability, including (a) before and (b) after views of a single family home on Fort Myers Beach constructed in 1950 that collapsed during Hurricane Ian; (c) before and (d) after views of two homes with disparate performance on Fort Myers Beach. Home (1) was constructed in 1956, while home (2) was constructed in 1950, but home (2) was elevated approximately 3 ft higher than home (1) and its breakaway walls performed as intended.

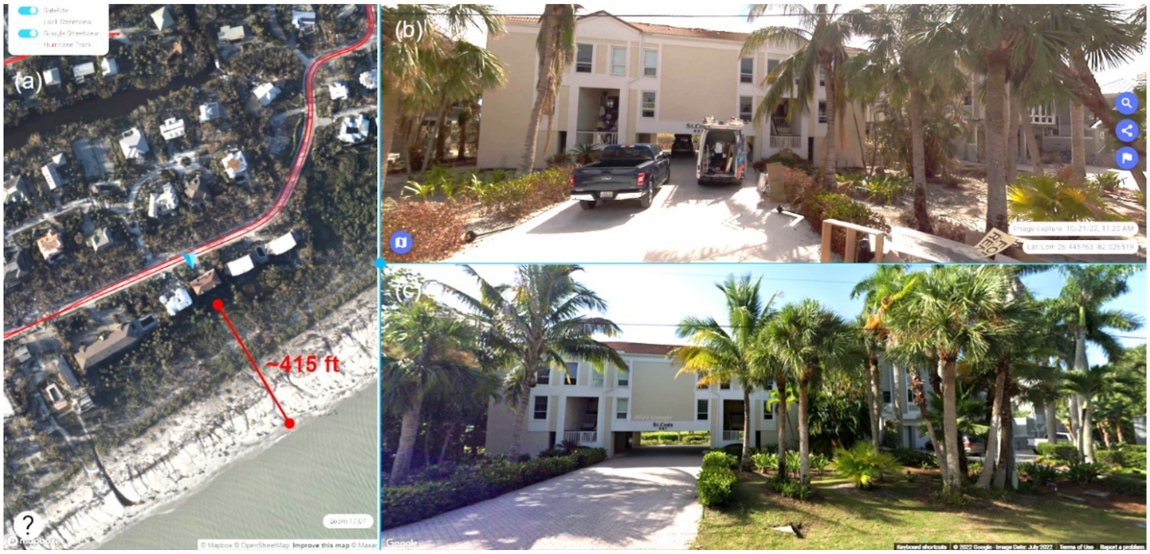

Figure 4.2. Illustrative effect of the vegetation and extended setback in Sanibel potentially mitigating surge impacts to structures. Subset (a) provides the post-storm aerial view showing a setback of approximately 415 ft from the shoreline, (b) the post-storm surface-level view, and (c) the pre-storm surface-level view.

Figure 4.3. Examples of the performance of breakaway walls during Hurricane Ian, including (a) before and (b) after views of a home on Fort Myers Beach constructed in 2000 with acceptable performance of the breakaway walls; and (c) before and (d) after views of a two-story structure with garage at ground level constructed in 2020 in which the breakaway CMU walls on the back side of the structure only partially broke away.

Figure 4.4. Examples of scour, uplift, and other surge effects on buildings during Hurricane Ian, including (a) debris transport and breakaway wall performance, (b) scouring and pavement washout, (c) scour around piers, and (d) effects of hydrodynamic uplift forces on a wood-framed floor system.

Figure 4.5. Illustrative performance of critical or cultural facilities on the barrier islands, including (a) the Ft. Myers Beach Fire Department District Station 31, constructed in 1985 with partial collapse of some walls and breaching of roll-up doors; (b) the Ft. Myers Beach Library (portion shown added in 2011) with only minor loss of metal roof cover visible (not shown); (c) Ft. Myers Beach Town Hall (constructed in 1968) with surge damage to end wall and washout below foundation; (d) Ft. Myers Fire Station No. 33 (built in 2008) with no visible signs of exterior damage; (e) Pine Island Fire Station (built in 1975) with no signs of exterior damage; and (f) Sanibel Fire Department Station 171 (built in 2005) with no visible signs of exterior damage.

Figure 4.6. Examples of poor wind performance on the barrier islands, including (a) a 3-story home constructed in 1999 with partial roof structure removal and wall collapse in the top story, (b) gable end roof structure loss in apartment buildings constructed in 1986; (c) garage door framing blown inward in a home constructed in 1967; (d) roof structure failure in one home adjacent to loss of metal roof cover in another, both of which were constructed in 1978.

Figure 4.7. Example of surge impacts on RVs and manufactured homes on Ft. Myers Beach during Hurricane Ian: (a) before oblique view of the RV park, and (b) after view of the RV park shown in (a). The red triangle in (a) approximates the location and field of view in (b).

4.2. Coastal Urban Regions (Cape Coral, Ft. Myers, Port Charlotte, Punta Gorda)

Coastal urban regions such as Cape Coral, Ft. Myers, Port Charlotte and Punta Gorda experienced primarily high wind, flooding (both surge-induced and rain-induced), and heavy rain hazards. Missing was the wave action that contributed heavily to the damages observed in the barrier islands. Structures as a whole appear to have performed well in what was ultimately a below design-level event for wind hazards based on the preliminary wind field modeling (Cortes et al., 2022). The following summarizes some key observations taken from review of the NOAA aerial imagery and the SLP and other imagery collected by FAST-1.

- **Isolated structural wind damage was observed in Punta Gorda, Port Charlotte and surrounding regions**, primarily consisting of the loss of structural roof framing (e.g., rafters, trusses, purlins) in older construction (pre-Florida Building Code) as illustrated in Figure 4.8. Structural damage to site-built single-family homes was isolated in these areas, as a preliminary review of the FAST-1 imagery did not reveal any examples of such failures.

- **Roof cover damage was commonly observed but the extent of damage varied considerably.** The frequency and extent of damage by roof cover material type is beyond the focus of this EARR, but examples of damage were easily identified for asphalt shingle (Fig. 4.9) and clay/concrete tile (Fig. 4.10) roofs. Older asphalt shingle roofs tended to experience the most severe damage, while newer asphalt shingle roofs and tile roofs typically only exhibited the loss of a few shingles or tiles, respectively. Many non-residential buildings also showed signs of roof cover damage, including hospital facilities as highlighted in Cortes et al. (2022).

- **Municipal structures performed well, showing only minor damage to building envelope components (roofing, wall cladding)** (Fig. 4.11). For example, the Peace River Elementary School in Punta Gorda appeared essentially unscathed save for failure of metal trellis (Fig. 4.11a).

- **A few illustrative examples of significant fenestration damage were observed** (Fig. 4.12), but such damage also does not appear to be widespread.

- **Manufactured home communities' performance was generally worse than that of site-built construction, but structural damage was still not common in the coastal urban regions**. Damage primarily consisted of the loss of cladding elements, as illustrated in Figure 4.13, but structural damage was more frequently observed in some communities closer to the coast where the highest wind speeds would have been experienced (Fig. 4.13 a,b).

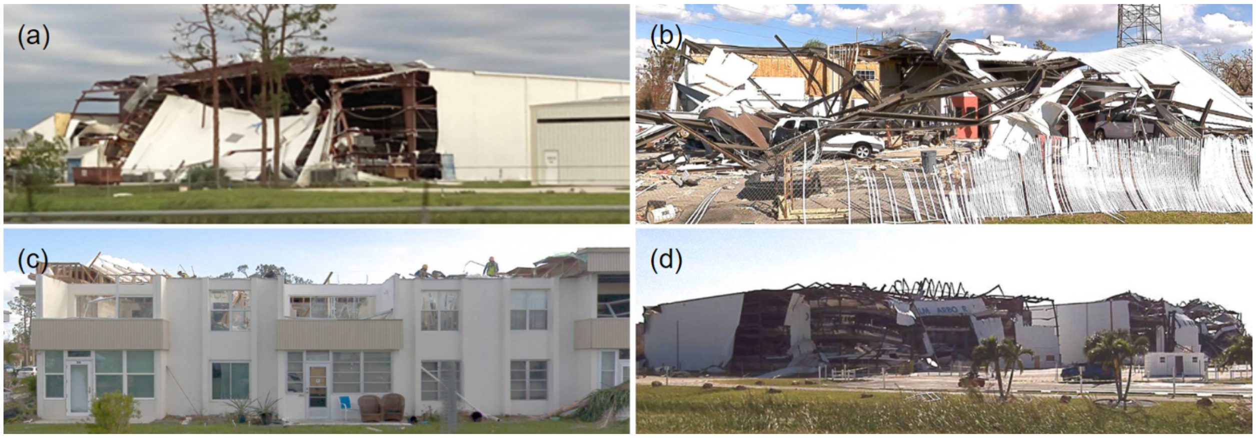

Figure 4.8. Examples of significant structural damage from Hurricane Ian, including (a) end bay failure in a metal building aircraft hangar (year built: 1996) at Punta Gorda airport, (b) collapse of an automobile maintenance garage in Grove City constructed in 1986; (c) wood roof structure failure in two-story wood-frame condominiums in Port Charlotte constructed in 1973, and (d) end bay collapses and cladding loss of two marina buildings in Cape Haze constructed in 1999.

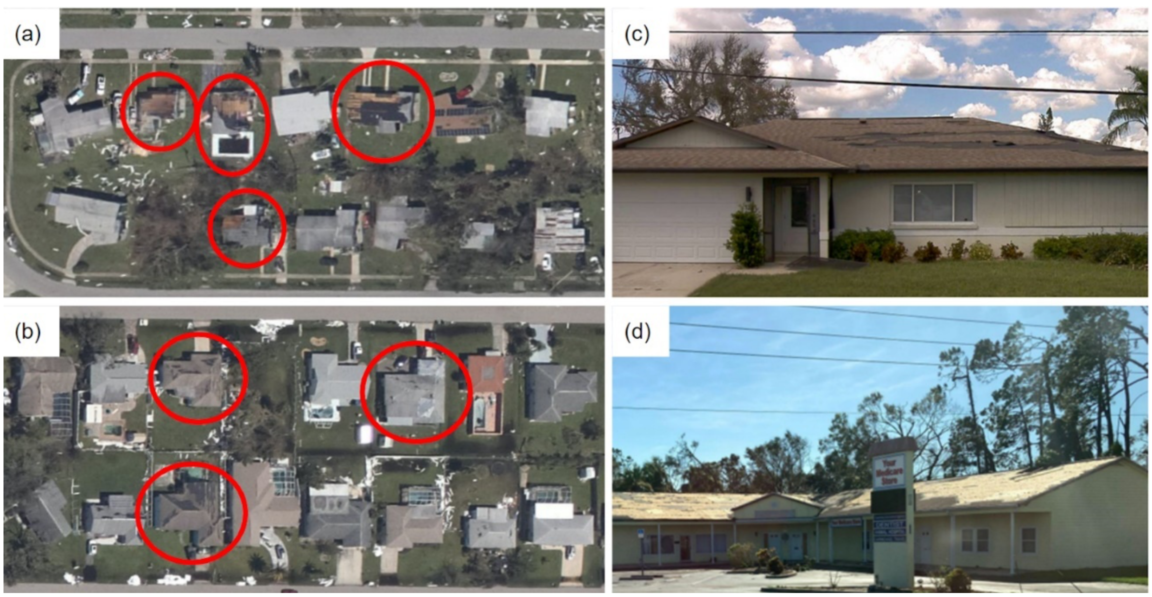

Figure 4.9. Illustrative performance of asphalt shingle and rolled membrane roofs in Port Charlotte consisting of homes constructed in the (a) 1960s with asphalt shingles and rolled roofs, (b) 1980s, (c) 1980s construction but asphalt shingle roof installed in 2005 but also (d) isolated commercial structures.

Figure 4.10. Illustrative examples of damage to tiled roofs, including (a) tile uplift (indicated by red ellipses) concentrated along the eaves of a single family home in Punta Gorda constructed in 1969; (b) loose tiles in the field and ridge regions of the roof on a condominium in Punta Gorda, FL constructed in 1989; and (c) isolated loose tiles on a roof on a multi-family residential unit also in Punta Gorda, FL constructed in 1990.

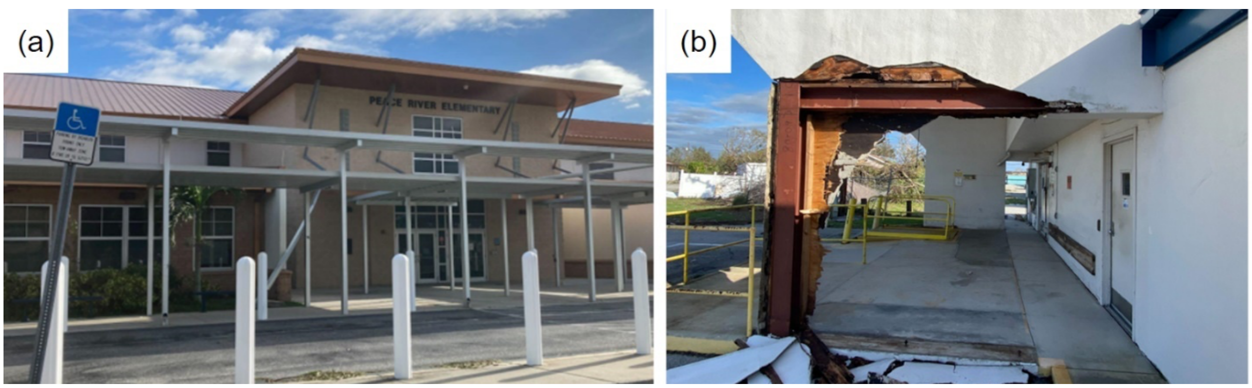

Figure 4.11. Isolated cladding loss in non-residential buildings, including (a) minor damage to flashing at Peace River Elementary School in Port Charlotte and (b) failure of exterior stucco-clad wall panel at USPS office in Port Charlotte.

Figure 4.12. Examples of isolated fenestration damage observed in the Port Charlotte area, including (a) and (b) complete loss of glass storefront in a commercial building constructed in 1973 , and (c) broken windows in a 5-story commercial building constructed in 1987.

Figure 4.13. Illustrative damage to mobile/manufactured homes, including (a) aerial and (b) street-level views of structural damage to Gasparilla Mobile Estates in Placida (established in the 1970s), including loss of roof structure and wall collapses; (c) cladding damage to manufactured homes in Punta Gorda; and (d) shifted unreinforced masonry piers supporting a manufactured home subjected to storm surge on San Carlos Island.

4.3. Inland Regions

FAST-1 did not observe any significant structural damage in the inland regions during limited scouting, primarily while traveling to/from home bases and the coastal urban regions of interest.

A few illustrative photos of inland flooding and damage to transportation infrastructure captured by FAST 1.1 are shown in Figure 4.14. While Hurricane Ian caused significant impacts in these inland areas due to flooding, tree-falls, and other hazards, the impacts are likely outside of the purview of StEER and are not investigated further at this time.

Figure 4.14. Photos of damage to the road infrastructure in inland regions: (a) street flooding at Exit 182 in I-75 on route to Sumter Blvd. and (b) damaged traffic lights at the intersection of City Center and Sumter Blvd. in the city of North Port.

Appendix B References

ARA. 2022. *Hurricane Ian Landfall in FL Peak Gust Wind Speeds (Release 3)*. Applied Research Associates.

Cortes, M., P. Arora, L. Ceferino, H. Ibrahim, D. Istrati, D. Reed, D. Roueche, A. Safiey, T. Tomiczek, I. Zisis, M. Alam, T. Kijewski-Correa, D. Prevatt, and I. Robertson. 2022. "StEER: Hurricane Ian Preliminary Virtual Reconnaissance Report (PVRR)." Designsafe-CI. DOI: 10.17603/DS2-KC9K-S242

Kijewski-Correa, T., D. Prevatt, D. Roueche, I. Robertson, M. Alam, A. Safiey, I. Zisis, O. Lafontaine, O. Nofal, L. Rhode-Barbarigos, A. Subgranon, D. Faraone, J. Micali, J. X. Santiago-Hernández, and D. Agdas. 2023. "StEER: Hurricane Ian Early Access Reconnaissance Report (EARR)." Designsafe-CI. DOI: 10.17603/DS2-3PC2-7P82

Appendix B Figure Metadata

Figure ID	Latitude	Longitude	Source of Photo
Figure 4.1(a)	26.4265	-81.9093	Google Maps
Figure 4.2(b)	26.4265	-81.9093	StEER FAST 1.3
Figure 4.1(c)	26.4356	-81.9198	Google Maps
Figure 4.1(d)	26.4356	-81.9198	StEER FAST 1.3
Figure 4.2(a)	26.4457	-82.0265	NOAA

Figure 4.2(b)	26.4457	-82.0265	StEER FAST 1.3
Figure 4.2(c)	26.4457	-82.0265	Google Maps
Figure 4.3(a)	26.4312	-81.9142	Google Maps
Figure 4.3(b)	26.4312	-81.9142	StEER FAST 1.3
Figure 4.3(c)	26.4287	-81.9119	Google Maps
Figure 4.3(d)	26.4287	-81.9119	StEER FAST 1.3
Figure 4.4(a)	26.4332	-81.9159	Mohammmad Alam / StEER
Figure 4.4(b)	26.4222	-81.9057	Mohammmad Alam/ StEER
Figure 4.4(c)	26.4145	-81.9020	Mohammmad Alam/ StEER
Figure 4.4(d)	26.4545	-81.9582	Mohammmad Alam/ StEER
Figure 4.5(a)	26.4452	-81.9353	StEER FAST 1.3
Figure 4.5(b)	26.4479	-81.9391	StEER FAST 1.3
Figure 4.5(c)	26.4486	-81.9427	StEER FAST 1.3
Figure 4.5(d)	26.4153	-81.8999	StEER FAST 1.3
Figure 4.5(e)	26.5332	-82.0881	StEER FAST 1.3
Figure 4.5(f)	26.4381	-82.0776	StEER FAST 1.3
Figure 4.6(a)	26.5009	-82.0630	StEER FAST 1.3
Figure 4.6(b)	26.8101	-82.2757	StEER FAST 1.3
Figure 4.6(c)	26.6958	-82.1476	StEER FAST 1.3
Figure 4.6(d)	26.7333	-82.2625	StEER FAST 1.3
Figure 4.7(a)	26.4461	-81.9357	Pictometry Eagleview
Figure 4.7(b)	26.4461	-81.9357	StEER FAST 1.3
Figure 4.8(a)	26.9207	-82.0009	StEER FAST 1.3
Figure 4.8(b)	26.8985	-82.3117	StEER FAST 1.3
Figure 4.8(c)	26.9922	-82.0994	StEER FAST 1.3
Figure 4.8(d)	26.8699	-82.3086	StEER FAST 1.3
Figure 4.9(a)	26.99	-82.09	NOAA

Figure 4.9(b)	26.986	-82.078	NOAA
Figure 4.9(c)	26.621	-81.948	StEER FAST 1.3
Figure 4.9(d)	27.0174	-82.1573	StEER FAST 1.1
Figure 4.10(a)	26.9154	-82.0737	StEER FAST 1.3
Figure 4.10(b)	26.9054	-82.0733	StEER FAST 1.3
Figure 4.10(c)	26.9071	-82.0619	StEER FAST 1.3
Figure 4.11(a)	26.9691	-82.0774	StEER FAST 1.1
Figure 4.11(b)	26.9756	-82.0882	StEER FAST 1.1
Figure 4.12(a)	27.0152	-82.1528	StEER FAST 1.1
Figure 4.12(b)	27.0152	-82.1528	StEER FAST 1.1
Figure 4.12(c)	27.0075	- 82.1357	StEER FAST 1.1
Figure 4.13(a)	26.8375	-82.2598	StEER FAST 1.3
Figure 4.13(b)	26.8378	-82.2605	StEER FAST 1.3
Figure 4.13(c)	26.880	-82.024	StEER FAST 1.3
Figure 4.13(d)	26.4586	-81.942	StEER FAST 1.2
Figure 4.14(a)	27.0984	-82.2038	StEER FAST 1.1
Figure 4.14(b)	27.0737	-82.2091	StEER FAST 1.1

APPENDIX C. ON-SITE DEPLOYMENTS CONDUCTED BY STEER IN THE AFTERMATH OF HURRICANE IAN (2022)

Table C1. Deployments conducted by StEER in the aftermath of Hurricane Ian (2022).

Team Member	Affiliation	PA [1]	UAS [1]	HWM [1]
FAST 3.1: October 19-23, 2022 [1]				
Rob Davis	Plainsman Engineering	●		
Kurt Gurley	University of Florida	●		
Chris Rizer	Simpson Strong Tie	●		
Luis Ceferino	New York University	●		
Jean-Paul Pinelli	Florida Institute of Technology	●		
Zhuoxuan Wei*	Florida Institute of Technology	●		
Jaqueline Zdebski	University of Washington (RAPID EF)		●	
Mohammad Shafiq Alam	University of Notre Dame	●	●	
Joey Civello	Frontier Precision		●	
Pat Lynett	University of Southern California			●
Maile McCann*	University of Southern California			●
Ezgi Cinar*	University of Southern California			●
Willington Renteria*	University of Southern California			●
FAST 3.2: October 31-November 4, 2022				
James Kaihatu	Texas A&M University			●
Sabarethinam Kameshwar	Louisiana State University			●
Maile McCann*	University of Southern California			●
Behzad Ebrahimi*	University of Southern California			●
* denotes a student research assistant **PA** = Performance Assessment, **UAS** = Unmanned Aerial System, **HWM** = High Water Mark				

APPENDIX D. WIND AND SURGE DAMAGE RATINGS

Table D1. Surge damage ratings, following Friedland (2007).

Damage State	**Description**
0 None or Very Minor Damage	No floodwater impacts.
1 Minor Damage	Breakaway walls or appurtenant structures damaged or removed WITHOUT physical damage to remaining structure. No flood impacts the building.
2 Moderate Damage	Some wall cladding damage from flood-borne debris. Breakaway walls or appurtenant structures damage or removed WITH physical damage to remaining structures.
3 Severe Damage	Removal of cladding from "wash through" of surge without wall structural damage.
4 Very Severe Damage	Failure of wall frame, repairable structural damage to any portion of building, or < 25% of building plan area unrepairable.
5 Partial Collapse	Building shifted off foundation, overall structure racking, >25% of structure unrepairable.
6 Collapse	Total structural failure (no intact structure).

Table D2. Wind damage ratings, following Kijewski-Correa et al. (2020).

		Presence of Extent of Failure in:					
Damage State [1]	**Short Description**	**Roof or wall cover**	**Window or door**	**Roof or wall substrate**	**Roof structure**	**Wall structure [2]**	**Fascia and/or soffit**
0 No damage	No visible exterior damage	0%	No	No	No	No	No
1 Minor damage	Damage confined to envelope	**> 0% and ≤ 15%**	**1**	No	No	No	≤ 20%
2 Moderate damage	Load path preserved, but significant repairs required	**> 15% and ≤ 50%**	**> 1 and ≤ the larger of 3 and 20%**	**1 to 3 panels**	No	No	**> 20%**
3 Severe damage	Major impacts to structural load path	**> 50%**	**> the larger of 3 and 20% and ≤ 50%**	**> 3 and ≤ 25%**	**≤ 15%**	No	
4 Destroyed	Total loss. Structural load path compromised beyond repair	> 50%	**> 50%**	**> 25%**	**> 15%**	Yes	

Notes:
[1] A building is considered to be in the damage state if any of the if any of the bolded damage criteria in the corresponding row are met.
[2] Wall structure refers to the walls in the living area only. The ground floor of elevated structures often have breakaway walls that can be easily damage by storm surge. This damage should be ignored in assigning the overall damage rating.

APPENDIX E. LIST OF ATTRIBUTES AND FEATURES BEING COLLECTED IN THE DATA ENRICHMENT EFFORT.

The following provides a list and brief description of the building attributes and features being collected as part of the data enrichment effort of Task 5.1.

Features	Descriptions
ID	Unique identifier for each building
Latitude	GPS Latitude
Longitude	GPS Longitude
Occupancy	Occupancy class of building
Address Sub Thoroughfare	Street number
Address Thoroughfare	Street name
Address Locality	City
Address Sub Admin Area	County
Address Admin Area	State
Address Postal Code	Zip Code
Year Built	Original year of construction
Number of Stories	Number of stories above ground
Elevation to LHSM	Elevation to lowest horizontal structural member in feet
Base Flood Elevation	Base flood elevation as determined by the current FEMA FIRM
CCCL Location	Location inside or outside of the Coastal Construction Control Line
Wall Cladding Type 1	Primary wall cladding type
Wall Cladding Type 1 Area	Proportion of primary wall cladding type
Wall Cladding Type 2	Secondary wall cladding type
Wall Cladding Type 2 Area	Proportion of secondary wall cladding type
Roof Cover	Roof cover type
Roof Shape	Shape of roof
Mean Roof Height	Average height of roof in ft relative to grade
Building Length	Maximum horizontal footprint dimension
Building Width	Minimum horizontal footprint dimension
Foundation Type	Type of foundation system
Structural System	Type of primary structural system
Breakaway Wall Performance	Whether breakaway walls are present and if so, whether they failed or not
Flood Slab Uplift	Whether floor slab uplift is observed
Debris Impact Damming	Whether debris impact or damming is present or contributed to damage
Building Collapsed or Partially Collapsed	Whether building is partially or fully collapsed
Building Shifted Off Foundation	Whether building has been displaced off its foundation
Garage Door Performance	Whether garage door is present, and performance if so
Roof Structure Damage	Percentage of roof structure damaged or missing
Roof Substrate Damage	Percentage of roof decking damaged or missing
Roof Cover Damage	Percentage of roof cover damaged or missing
Wall Structure Damage	Percentage of wall structure damaged or missing

Wall Substrate Damage	Percentage of wall sheathing damaged or missing
Wall Cover Type 1 Damage	Percentage of primary wall cover type damaged or missing
Wall Cover Type 2 Damage	Percentage of secondary wall cover type damaged or missing
Fenestration Damage	Percentage of windows or entry doors damaged or missing
Soffit Damage	Whether soffit damage is observed
Fascia Damage	Whether fascia damage is observed
Surge Damage Rating	Overall surge damage rating
Wind Damage Rating	Overall wind damage rating
Permit 1 Number	Permit number for wind mitigation related permit
Permit 1 Type	Type of wind mitigation related permit
Permit 1 Year	Year permit was closed
Permit 2 Number	Permit number for second wind mitigation related permit
Permit 2 Type	Type of wind mitigation related permit
Permit 2 Year	Year permit was closed
Base Flood Elevation	Base flood elevation relative to NAV88 from the 2022 FEMA FIRMs
Flood Zone	Flood zone from the 2022 FEMA FIRMS
Ground Elevation	Bare-earth ground elevation relative to NAV88 from the USGS national elevation dataset.
Peak Gust Wind Speed	Peak estimated 3-second gust wind speed in mph from the ARA wind maps
Peak Sustained Wind Speed	Peak estimated 1-minute sustained wind speed in mph from the ARA wind maps
Storm Surge Inundation (HWM)	Peak storm surge inundation in ft relative to NAVD88 interpolated from high water marks collected by StEER and the USGS
Storm Surge Inundation (CERA)	Peak storm surge inundation in ft relative to grade level from hindcast ADCIRC modeling by the Coastal Emergency Risk Assessment.